Modular Representation Synthesis Framework for Homogeneous Azeotropic Separation

Soraya Rahim Ismail and Efstratios N. Pistikopoulos
Centre for Process Systems Engineering, Dept. of Chemical Engineering, Imperial College, London SW7 2BY

Katerina P. Papalexandri
Chemical Process Engineering Research Institute, FORTH, Thessaloniki, Greece

The synthesis and design of separation systems for nonideal azeotropic mixtures traditionally utilize graphical methods, focusing on separation feasibility within a sequential design framework. Once promising systems have been identified, sequencing and design are optimized in a second stage, limited by the separation feasibility region defined in the first stage. A generalized modular representation proposed for the synthesis of nonideal separations can simultaneously explore entrainer and sequencing alternatives. A multipurpose mass/heat exchange module, introduced in earlier work, is employed to investigate separation units and structures as mass- and heat-exchange possibilities. Process units, separation sequences, and entrainers that aid the separation are examined within one separation problem rather than in a sequential manner. Promising separation schemes can be further considered for detailed design optimization.

Introduction

As nonideal behavior has been mostly studied in a case-dependent manner, nonideal separations and corresponding synthesis methods are much less advanced than that for ideal separation systems. Currently there are no generally accepted rules or procedures to address sequencing of complex nonideal separations. Apart from the pioneering work of Doherty and his coworkers, there has been considerable recent activity in the development of systematic synthesis and design methodologies for azeotropic separations; Widagdo and Seider (1996), Westerberg and Wahnschafft (1996), and Biegler et al. (1997) give excellent reviews. A summary of such representative developments is shown in Table 1. A common feature of such advances is the emphasis on separation feasibility within a sequential framework typically based on analysis of residue curve maps and distillation lines. As shown, the synthesis problem has generally been decomposed into subtasks of entrainer selection, sequencing of columns, design, and optimization. Some of these works have been implemented into software codes, that is, MAYFLOWER (Malone and Doherty, 1994) and SPLIT (Wahnschafft et al., 1991, 1992b, 1993). Sequencing is limited by the separation feasibility region defined in the first stage of entrainer selection. A limitation to these approaches apart from their sequential nature is that the findings are not readily applicable to different separation technologies and hybrid systems, and thus nonconventional separation systems need to be studied separately.

In this work, a generalized modular framework is proposed by which entrainer and sequencing alternatives can be simultaneously explored in a single optimization problem. Fundamental heat and mass-transfer principles, coupled with detailed thermodynamic models, are employed within a mass/heat-exchange superstructure representation of process operations to investigate separation units and structures that are not explicitly prepostulated, while separation feasibility is consistently ensured.

The article is structured as follows. The following section formally states the synthesis problem. The mass/heat-transfer module and the corresponding mass-transfer constraints for the nonideal mixtures that constitute the basis for the synthesis representation are described in the third section. The synthesis framework is presented in the fourth section, with the mathematical model given in the fifth section, while two separation examples are considered in detail in the sixth section.

Correspondence concerning this article should be addressed to E. N. Pistikopoulos.

Table 1. Design Procedures

Authors	Features
	Entrainer Selection
Doherty and Caldarola (1985)	RCM, total reflux, ternary mixtures. Assumes linear distillation boundaries and no boundary crossing
Stichlmair et al. (1989)	DLM, total reflux, linear distillation boundaries
Foucher et al. (1991)	RCM, total reflux, ternary. Automatic procedure.
Laroche et al. (1991, 1992a)	RCM, ternary. Analysis based on ''equivolatility curves''
	Column Sequencing and Bounding Strategies
Laroche et al. (1992b)	RCM, all reflux, ternary. Separability in single-feed columns
Wahnschafft et al. (1992a)	RCM, all reflux, ternary mixtures, single-feed columns. Bounds by feed pinch-point trajectories
Fidkowski et al. (1993)	DLM, all reflux, ternary, single feed. Introduces ''distillation limit,'' accounts for boundary crossing, algebraic based
Stichlmair and Herguijuela (1992)	DLM, all reflux, ternary, single feed. Accounts for curved distillation boundaries
Jobson et al. (1995)	Achieves attainable product region based on simple distillation and mixing for ternary mixtures
Safrit and Westerberg (1997a,b)	RCM. Algorithm-determining boundaries and distillation regions for *n*-component systems
Rooks et al. (1998)	RCM. Equation-based approach to determine distillation region structures of multicomponent mixtures
	Design and Optimization
Boundary Value Design Procedure	
Levy et al. (1985)	Ternary mixtures, single-feed columns, CMO
Knight and Doherty (1986)	Ternary, single feed with heat effects
Julka and Doherty (1990)	Multicomponent, single feed, CMO. Tracks fixed points
Knapp and Doherty (1994)	Ternary, double-feed column, CMO. Calculates R_{min} and R_{max}
Fidkowski et al. (1991)	Up to 4 components, single feed, CMO. Algebraic continuation arc method to locate tangent pinch
Stichlmair et al. (1993)	Ternary mixture, ''pinch-point'' geometry
Bauer and Stichlmair (1995)	Combines pinch-point analysis with process MINLP optimization for ternary mixtures in single-feed columns
Castillo et al. (1998)	Introduces the concept of staged leaves for ternary mixtures in single feed
Bekiaris and Morari (1996)	Infinity/infinity analysis. Implications of multiplicities on synthesis and design

CMO—constant molar overflow; DLM—distillation line map; RCM—residue curve map.

Problem Statement

The separation synthesis problem addressed in this work can be stated as follows.

Given

- A multicomponent feed mixture of known nonideal behavior involving one or more azeotropes and given flow rate, composition, and temperature
- A set of products with desired specifications.
- A set of available entrainers that may facilitate the separation and form a *homogeneous* mixture with the feed components.
- Available heat utility streams such as steam and cooling water and specifications on availability, supply temperatures, and compositions.
- All thermodynamic property models.

Synthesize an optimal separation system, that is, sequence of separators and corresponding entrainer with respect to an overall separation cost. In this work, the separation cost comprises cost of utilities, cost of required separating agent, and an approximation of capital costs based on the number of mass/heat separators, as discussed later.

The basic assumptions in this work are

- The thermodynamic state of the feed and product streams are known. As a first analysis saturated liquid feeds and products are considered.
- Total pressure of the system is constant and specified.
- Heaters and coolers are assumed to be total reboilers and condensers, respectively.
- There is no heat integration between the heaters and coolers.

Within the proposed framework, all of these assumptions can be easily relaxed, as detailed later. However, they are imposed to restrict the size of the resulting mathematical model. Consider for example the separation of ethanol (A) and water (B). Ethanol (normal bp 351.44 K) and water (normal bp 373.15 K) form a minimum boiling azeotrope of 89.43 mol % ethanol at a temperature of 351.15 K and a pressure of 1 atm (Figure 1). Ethylene glycol (normal bp 470.45 K) is a heavy entrainer (H) and methanol (normal bp 337.8 K) a light entrainer (N), both of which can facilitate the separation by forming a homogeneous mixture with the feed.

Mass/Heat-Transfer Module

Broadly speaking, a process operation can be generally characterized by a set of mass- and heat-transfer phenomena, concerning mainly the mass transfer of a component from one substance or phase to another due to a difference in chemical potential. For example, in distillation, mass and heat are transferred between the contacting liquid and vapor phases of a mixture on a tray. To capture the mass- and heat-transfer phenomena in chemical processes, a mass- and

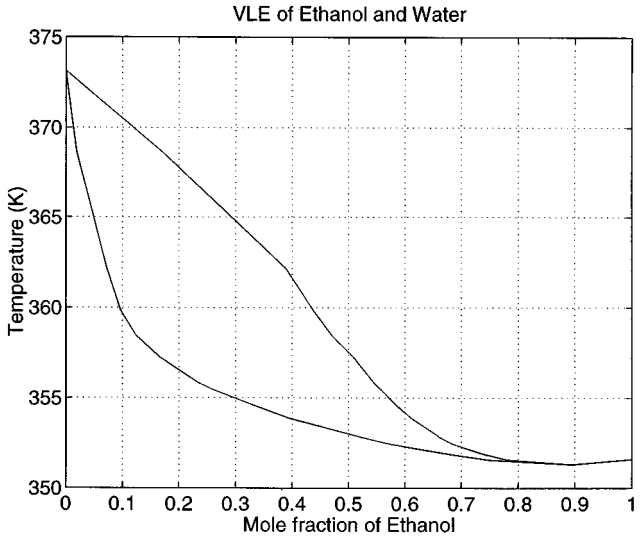

Figure 1. Vapor–liquid equilibrium for ethanol–water at 1 atm.

heat-transfer module is proposed to form the basic building block of a network superstructure of process alternatives (see Figure 2a) consisting of a mass/heat-exchange block, where mass and heat transfer takes place between the participating streams, connected to a pure heat-exchange block, where streams do not come into "mass active" contact (Papalexandri and Pistikopoulos, 1996). For simplification purposes in this work, no stream heat integration is considered, and the mass/heat-exchange block is connected to two utility exchangers, a heater and a cooler, as shown in Figure 2b. Side mixers and splitters are assigned to each mass/heat-exchange module, heater and cooler, and block-superstructure rules are applied allowing for all possible interconnections between exchangers.

In this way, process units can be represented by sets of properly connected mass- and heat-exchange blocks (Papalexandri and Pistikopoulos, 1996). For example, a distillation column with a total condenser and reboiler for the separation of a binary mixture A and B can be realized as two mass/heat-exchange blocks that represent the rectifying and stripping sections, connected to two pure heat-exchange blocks representing the condenser and reboiler (Figure 3). In both mass/heat-exchange blocks, A is transferred from the liquid to the vapor stream, and B is transferred from the vapor to the liquid stream. The condenser is realized as a pure heat-transfer block between an inlet vapor stream and a cooling utility, whereby thermodynamic constraints ensure that the inlet stream is of vapor phase, which is cooled to a liquid outlet stream. Similarly a reboiler is realized as heat exchange between a hot utility stream and an inlet liquid-phase stream that is heated to a vapor phase (see Papalexandri and Pistikopoulos (1996) for details).

Within a mass/heat-exchange block, mass transfer takes place when the two participating streams are not at equilibrium. This is ensured by imposing a set of mass-transfer "driving force" constraints at the inlet and outlet of the block (similar to the ΔT_{min} constraints in the pure heat-exchange case). In a $L_{AB} - V_{AB}$ mass/heat-exchange block (see Figure 4a), A is transferred from L_{AB} to V_{AB} when the liquid composition is greater than the equilibrium composition, that is,

$$\mathcal{G}1_c \geq 0$$
$$\mathcal{G}2_c \geq 0,$$

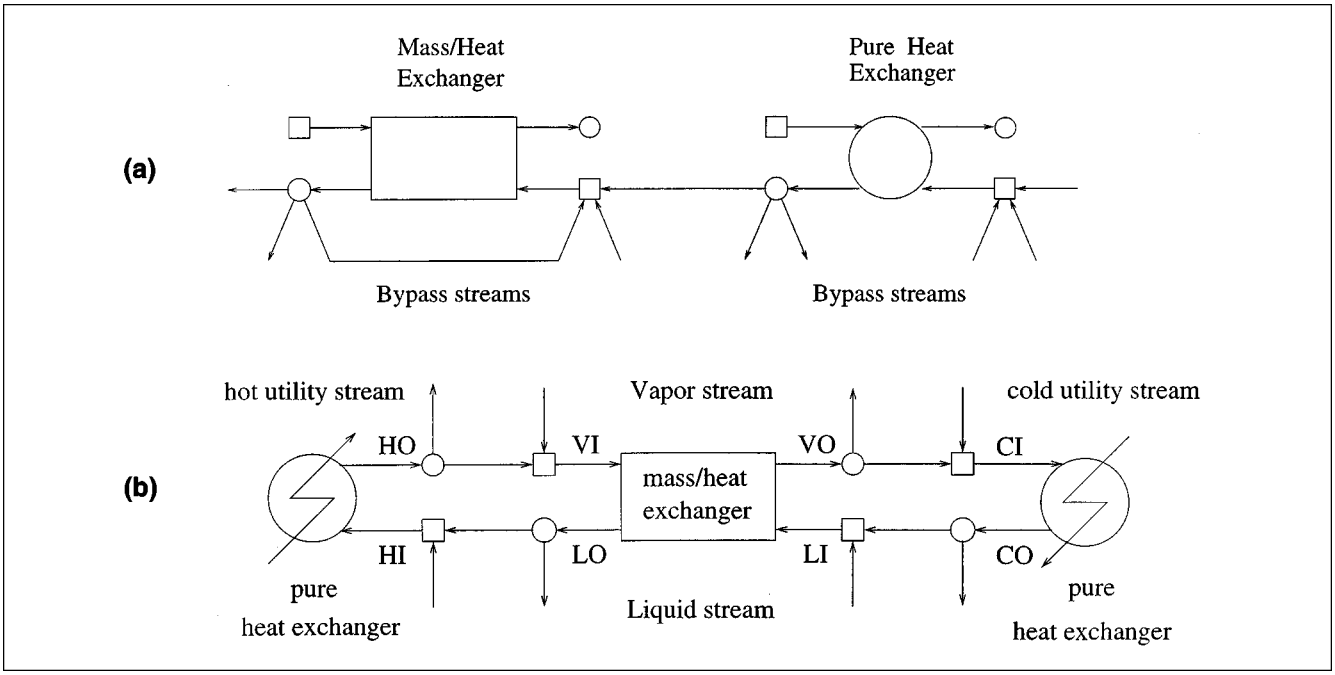

Figure 2. Mass/heat-exchange block.

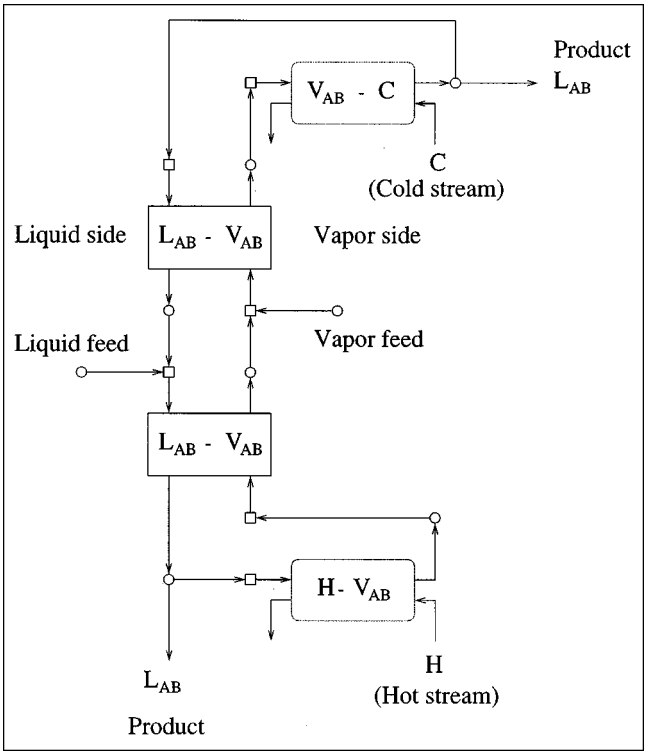

Figure 3. Binary distillation column.

where

$$\mathcal{G}1_c = K_c^{LI} x_c^{LI} - x_c^{VO} \quad (1)$$

$$\mathcal{G}2_c = K_c^{LO} x_c^{LO} - x_c^{VI}. \quad (2)$$

For the reverse case (see Figure 4b), A is transferred from V_{AB} to L_{AB}, and

$$\mathcal{G}1_c \le 0$$

$$\mathcal{G}2_c \le 0.$$

For the general case, when the mass-transfer direction is to be determined, we have

$$\mathcal{G}1_c * \mathcal{G}3_c \ge 0$$

$$\mathcal{G}2_c * \mathcal{G}3_c \ge 0, \quad (3)$$

where

$$\mathcal{G}3_c = f^{LI} x_c^{LI} - f^{LO} x_c^{LO} \quad (4)$$

denotes the *mass-transfer direction.* Note that in either transfer direction ($\mathcal{G}3_A \ge 0$ when A is transferred from liquid to vapor, and $\mathcal{G}3_A \le 0$ when A is transferred from vapor to liquid), mass transfer is consistently limited by Eqs. 3 (see Appendix A for detailed derivation). $\mathcal{G}1_c$ (Eq. 1) and $\mathcal{G}2_c$ (Eq. 2) represent how far away the liquid and vapor streams are from phase equilibrium, that is, the *distance from equilibrium.* When the liquid and vapor streams are at equilibrium, that

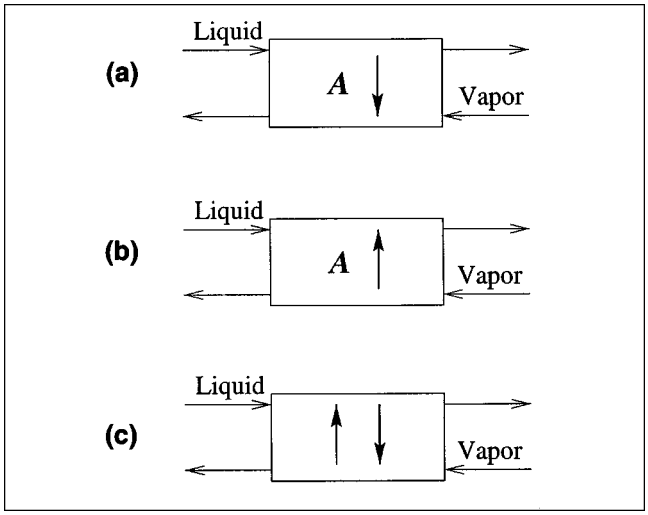

Figure 4. Mass transfer in mass/heat-exchange block.

is, when $\mathcal{G}1_c = \mathcal{G}2_c = 0$, no mass transfer occurs within the module that is, $\mathcal{G}3_c = 0$, and thus the module is redundant.

The mass-transfer directions of each component at the inlet and outlet of the module describes the mass-transfer pattern *within* the module. Due to the nonconvex nature of the constraints, it is noted that mass-transfer feasibility within the module may be violated (although satisfied at each end of the module) due to a double crossing of equilibrium. This may be overcome by aggregating each module to ensure feasibility in an inner loop algorithm. Within this work, postanalysis is conducted to ensure that infeasible mass transfer does not occur.

When the relative volatility of the mixture components are known, the bilinear constraints (Eqs. 3) are not necessary and the appropriate directional constraints are imposed on the individual components. For example, in the binary mixture AB, if A is more volatile than B, A will be transferred from the liquid to the vapor stream and B from the vapor to the liquid stream, and it holds that

$$\mathcal{G}2_A \ge 0 \qquad \mathcal{G}2_B \le 0$$

$$\mathcal{G}3_A \ge 0 \qquad \mathcal{G}3_B \le 0.$$

For general multicomponent nonideal systems, however, the constraints (Eqs. 3) do not require prepostulation of mass-transfer direction, which is an important feature, accounting for phenomena such as:

- In nonideal systems, the relative volatility, and thus mass-transfer direction, can depend on the mixture conditions (composition, temperature, and pressure).
- For azeotropic separation, the effect of the entrainer alters the relative volatility of the mixture, and therefore mass-transfer direction depends on the entrainer selected.
- For general separation systems, the constraints are able to model direct/indirect splits and also nonsharp splits.

To avoid the nonlinear, nonconvex constraints in Eqs. 3, a set of binary variables to denote the mass-transfer direction of each component in each mass/heat-exchange block e can

be introduced, that is,

$$yt_{ec} = \begin{cases} 1, & \text{when } c \text{ is transferred from liquid} \\ & \text{to vapor in mass/heat exchange } e \\ 0, & \text{when } c \text{ is transferred from vapor to liquid} \\ & \text{in mass/heat exchange } e, \end{cases}$$

enabling feasible mass transfer to be captured with the following set of mixed-integer constraints

$$\begin{aligned} (yt_{ec}-1)\mathfrak{U} \le \mathfrak{G}1_c \le yt_{ec}\mathfrak{U} \\ (yt_{ec}-1)\mathfrak{U} \le \mathfrak{G}2_c \le yt_{ec}\mathfrak{U} \\ (yt_{ec}-1)\mathfrak{U} \le \mathfrak{G}3_c \le yt_{ec}\mathfrak{U}, \end{aligned} \tag{5}$$

where $\mathfrak{U}$ is a (large) positive number. Note, for example, that when a component A is transferred from the liquid to the vapor in a module, $yt_A = 1$, and thus

$$\begin{aligned} 0 \le \mathfrak{G}1_A \le \mathfrak{U} \\ 0 \le \mathfrak{G}2_A \le \mathfrak{U} \\ 0 \le \mathfrak{G}3_A \le \mathfrak{U}, \end{aligned}$$

which is consistent with the previous discussion, and with constraints (Eqs. 3) (and similarly for when $yt_A = 0$).

Nonideal behavior can be captured employing detailed thermodynamic models for the calculation of the vapor–liquid equilibrium, that is,

$$K_c = \frac{\gamma_c P_c^{\text{sat}}}{\phi_c P_{\text{tot}}},$$

where the liquid-phase activity coefficient, γ_c, the vapor-phase fugacity coefficient, ϕ_c, and the vapor pressure can be calculated by appropriate thermodynamic models (such as UNIQUAC and NRTL).

Consider, for example, the separation of the ethanol and water mixture as described earlier, in a configuration of 20 mass/heat-exchange blocks that simulates a distillation column (see Figure 5). Maximizing the ethanol concentration of the distillate results in the azeotropic mixture of 89.8% ethanol concentration, verifying that the mass-transfer driving-force constraints properly capture the thermodynamic limitation (of the azeotrope).

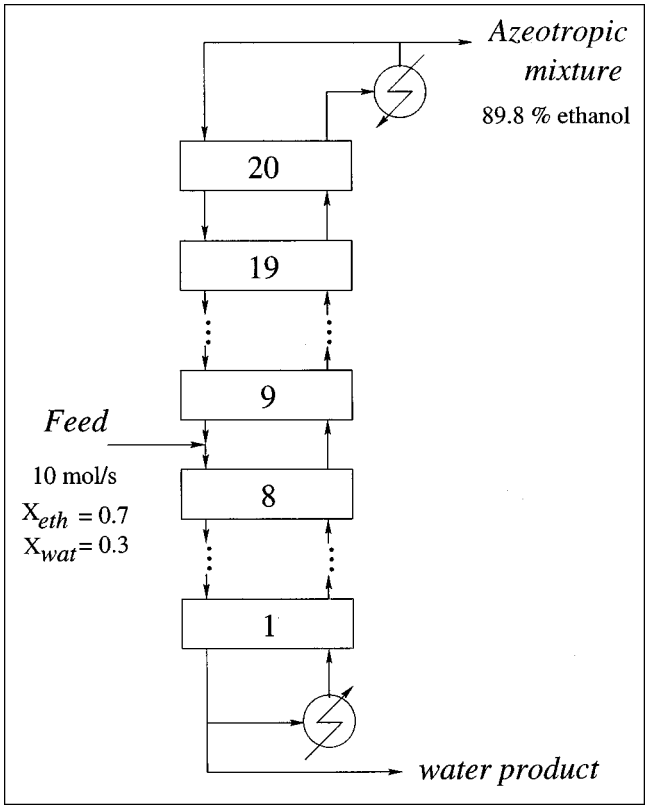

Figure 5. Separation of ethanol–water mixture.

Synthesis Framework

The main feature of the mass/heat-exchange modular synthesis framework is that all feasible alternatives are considered in a mass/heat superstructure. This framework includes the following.

Stream superset

A stream superset is constructed to account for all possible initial, intermediate, and final streams that may exist in a process. Defining a stream by its phase, a general mixed stream containing all components concerned in all possible phases is considered. For homogeneous mixtures, only liquid and vapor streams are of interest.

Revisit the separation of an azeotropic system AB whose separation can be facilitated by the addition of either a light entrainer N or a heavy entrainer H. The stream superset consists of a liquid and vapor mixed stream L_{NABH} and V_{NABH}, which accounts for all possible streams as follows:

- The binary feed stream is an instance of the liquid mixed stream L_{NABH} with $x_N = x_H = 0$.
- The feed of the light entrainer by setting

$$x_N = 1, \qquad x_A = x_B = x_H = 0.$$

All possible intermediate streams are also considered in a similar fashion.

Mass/heat-exchange matches

Stream matches are considered between streams where mass and/or heat transfer can occur. For the separation of a *homogeneous* mixture where no reaction occurs, mass transfer can only take place due to volatility differences between the liquid and vapor streams. Therefore only the liquid/vapor stream matches are considered. Possible mass-transfer directions for each component in a multicomponent mixture define more than one mass exchange pattern, thus multiple liquid/vapor matches corresponding to multiple mass/heat-exchange modules are considered.

For the case of the binary system AB, multiple matches corresponding to mass transfer of A from the liquid to the

vapor and that of B from the vapor to the liquid are considered, represented by

$$L_{AB} \underset{B}{\overset{A}{\rightleftharpoons}} V_{AB}.$$

For a multicomponent system, such as $NABH$ for the separation of ethanol and water described earlier, multiple $L_{NABH} - V_{NABH}$ matches are considered to allow for alternative mass-transfer direction (and thus structures). Assuming, for example, $N > A > B > H$ in terms of volatility, we may have

$$\text{(I)}\quad L_{NABH} \underset{ABH}{\overset{N}{\rightleftharpoons}} V_{NABH} \qquad \text{(II)}\quad L_{NABH} \underset{BH}{\overset{NA}{\rightleftharpoons}} V_{NABH} \qquad \text{(III)}\quad L_{NABH} \underset{H}{\overset{NAB}{\rightleftharpoons}} V_{NABH}.$$

Matches of type (I) corresponds to a N/ABH split, matches of type (II) to a NA/BH split, and so on.

Each liquid/vapor match represents a part of or a whole of a separator unit, which could be, for example an aggregate of distillation trays, or part of or whole of a packed column. Each liquid/vapor mass/heat-transfer module features a certain mass-transfer pattern, and the number of modules selected in the final solution reflects the differing mass-transfer patterns.

Note, however, that mass-transfer direction for each component, and thus order of volatility, is *not* prepostulated in the considered matches (as discussed in the previous section). This is of particular importance for nonideal separation whereby the order of volatility may change depending on the entrainer used.

Mass/heat-exchange network superstructure model

A superstructure is developed considering

- An initial splitter for each initial (feed) stream, from where flows are directed to the mixers of the modules that correspond to streams of the same phase and final mixers of product streams.
- A final mixer for each possible product stream, to where flows from the outlet splitters of the mass/heat-exchange modules (that correspond to streams of the same phase) and initial stream splitters are merged toward a final product flow.
- Interconnecting streams between the splitters and mixers of the mass/heat-exchange modules. Only streams of the same phase are allowed to mix.

This is illustrated in Figure 6 for $I = 1$ initial splitters (liquid), $P = 1$ final products (liquid), and $e = 3$ mass/heat modules. Logic is applied to screen out interconnections that cannot exist, thereby resulting in a reduced superstructure. This should not imply any bias toward the final solution, but rather screen out any physically undesirable interconnections for the system, that is, recycling of a stream that has just been separated is illogical and not allowed. The mathematical model for the resulting network is formulated as a mixed-integer nonlinear problem (MINLP), consisting of mass and energy balances, mass-transfer driving force constraints, phase-defining constraints for each stream, logical constraints to fathom out infeasible structures, and an objective function. The mathematical model is described in the next section, and detailed in Appendix B.

Table 2. Structural Variables

Variable	Denoting the Existence of
yh_e	Utility heater prior to vapor inlet of module e
yc_e	Utility cooler prior to liquid inlet of module e
$yll_{ee'}$	Interconnecting stream from liquid outlet splitter of module e to liquid inlet mixer of module e'
$yvv_{ee'}$	Interconnecting stream from vapor outlet splitter of module e to vapor inlet mixer of module e'
$ylh_{ee'}$	Liquid stream from liquid outlet splitter of module e to utility heater of module e'
$yhv_{ee'}$	Vapor stream from utility heater of module e to vapor inlet mixer of module e'
$yvc_{ee'}$	Vapor stream from vapor outlet splitter of module e to utility cooler of module e'
$ycl_{ee'}$	Interconnecting stream from utility cooler of module e to liquid inlet mixer of module e'
yIl_{ne}	Interconnecting stream from initial splitter of stream n to liquid inlet mixer of module e
yIh_{ne}	Interconnecting stream from initial splitter of stream n to utility heater of module e
yIp_{np}	Interconnecting stream from initial splitter of stream n to final mixer of product stream p
ylp_{ep}	Interconnecting stream from liquid outlet splitter of module e to the final mixer of product stream p
ycp_{ep}	Interconnecting stream from outlet utility cooler of module e to the final mixer of product stream p

Mathematical Model

Binary variables are introduced to denote (i) the existence (or not) of each module, (ii) existence (or not) of interconnecting streams between the splitters and mixers, and (iii) the mass-transfer direction for each component in each module. Note that variables (ii) are not necessary; thus, their presence does not increase the combinatorial complexity of the synthesis problem. They are utilized to simplify the solution of the nonlinear part of the superstructure model and to facilitate the introduction of logical constraints to the model. Similarly, variables (iii) are not necessary and their inclusion simplifies the mass-transfer driving-force constraints.

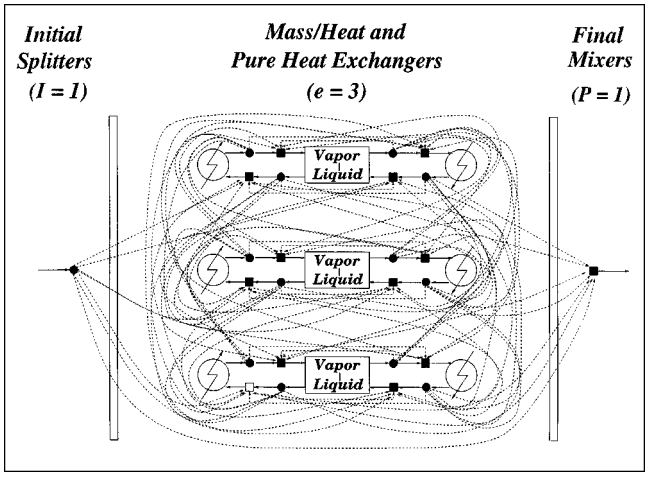

Figure 6. Illustrative superstructure network.

The mass/heat-exchange network superstructure model is formulated as a mixed-integer optimization problem (MINLP), involving the following:

- Total mass balances at all splitters and mixers of the superstructure.
- Component mass balances at all mixers and around the mass/heat and pure-heat exchangers.
- Energy balances at all mixers and around the pure-heat and mass/heat exchangers assuming adiabatic stream mixing.
- Summation of stream molar fractions.
- Phase-defining constraints for each stream, ensuring that the temperature of liquid streams is at most the mixture boiling point (bubble point), and that of vapor streams are at least the mixture dew point.
- Driving force constraints at mass/heat exchangers as detailed earlier.
- Physical property models.
- Mixed-integer constraints to account for the existence of modules and interconnections.
- Pure integer constraints corresponding to logical conditions or process constraints, reducing combinatorial complexity.
- Objective function, including the cost of entrainer, heat utilities, and fixed cost of the module.

The full mathematical model is detailed in Appendix B and corresponds to a large-scale MINLP problem, for which a nested MINLP decomposition strategy is developed for its solution (Appendix C). The model is solved using GAMS (Brooke et al., 1988), with solvers CONOPT employed for the primal problem and CPLEX for the master problems. Appendix D gives the size statistics of the model for the example problems described in the next section. The complexity and size of the model increases with the total number of mass/heat modules e considered. In solving the MINLP, a conservative number of modules is considered and if all modules are selected, this number is increased. With the problems considered in this work, it is found that a maximum of ten is sufficient.

Note that there is no prespostulation of the type of units used. The superstructure of mass/heat-transfer modules is optimized, and an equivalent process flowsheet is then derived from the final structure of mass/heat-transfer units obtained.

Examples

In this section, the separation task for two azeotropic mixtures are considered in detail to illustrate the ability of the proposed synthesis framework to

1. Consistently characterize separation feasibility
2. Identify the requirement (or not) of an (simultaneously depicted) entrainer
3. Determine the separation structure.

Utility cost data are as given in Table 3. Note that for convenience in the presentation, we make a number of simplifying assumptions:

1. Saturated liquid feeds and liquid products are considered.
2. The system is at constant atmospheric pressure.

Table 3. Utility Cost Data

Utility	Cost US$ per kWyr
Cooling Water	26.19
Steam	137.27

3. No heat integration between the separators is considered.

As discussed, these assumptions can be easily relaxed.

Example 1: separation of ethanol and water

For the separation of the ethanol (A) and water (B) mixture introduced earlier, ethylene glycol and methanol are considered as available candidate entrainers. Methanol (N) is a light entrainer with a lower boiling point than the azeotrope and introduces no new azeotrope, thus coming under case 020 under the entrainer classification of Doherty and Caldarola (1985). All the residue curves start from the methanol corner and end at a pure ethanol or water vertex, and a residue curve boundary runs from the entrainer to the minimum boiling azeotrope (see Figure 7a). Entrainers of this

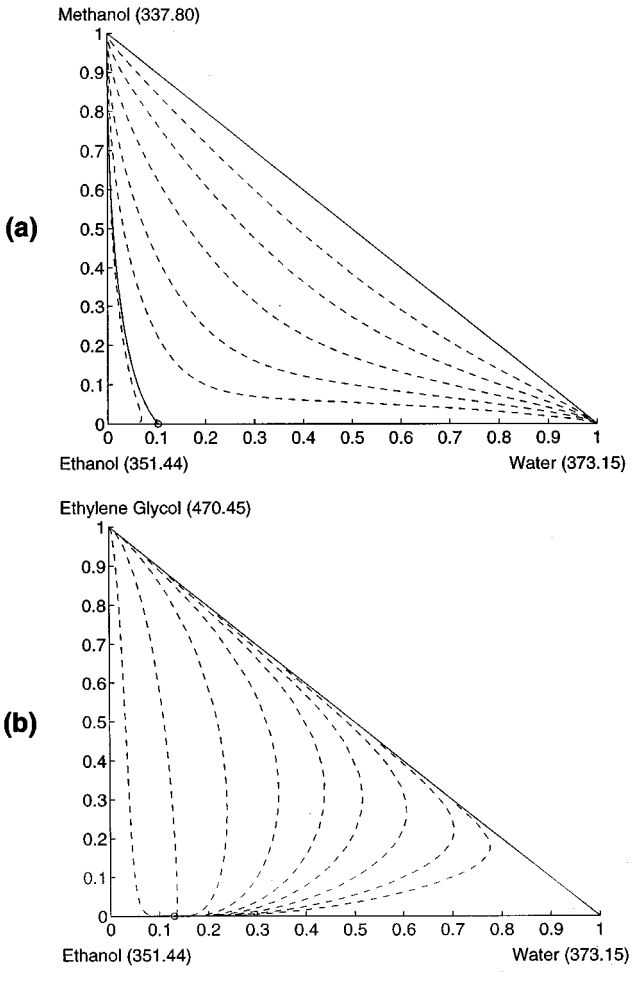

Figure 7. Residue curve maps for ethanol–water at 1 atm.

(a) Ethanol, water, and methanol mixture. (b) Ethanol, water, and ethylene glycol mixture.

Table 4. Ethanol–Water Separation: Thermodynamic Properties

	C1	C2	C3	C4	C5
Ethanol (1)	59.796	−6,595.0	−5.0474	$6.300e-7$	2
Water (2)	72.550	−7,206.7	−7.1385	$4.046e-6$	2
Ethylene glycol (3)	194.64	−14,615	−25.433	$2.014e-5$	2
Methanol (4)	109.93	−7,471.3	−13.988	$1.528e-2$	1

$$\ln P^{\text{sat}} = C1 + \frac{C2}{T} + C3\ln(T) + C4\,T^{C5} \quad \text{(Pa, K)}$$

NRTL Equation

$$\ln \gamma_i = \frac{\sum_{j\in C}\tau_{ji}G_{ji}x_j}{\sum_{j\in C}G_{ji}x_j} + \sum_{j\in C}\frac{G_{ij}x_j}{\sum_{l\in C}G_{lj}x_l}\left\{\tau_{ij} - \frac{\sum_{l\in C}\tau_{lj}G_{lj}x_l}{\sum_{l\in C}G_{lj}x_l}\right\}$$

$$\tau_{ij} = \frac{\Lambda_{ij}}{RT} \qquad G_{ij} = \exp(-\alpha_{ij}\tau_{ij})$$

$$\Lambda ii = 0 \qquad \alpha_{ij} = \alpha_{ji}$$

Ethanol–Water System

$\Lambda_{12} = 121.0$ cal/mol $\quad \Lambda_{21} = 1{,}161.5$ cal/mol $\quad \alpha_{12} = 0.475$

Ethanol–Water–Ethylene Glycol System

$$\Lambda_{ij} = \mathfrak{a}\mathfrak{a}_{ij} + \mathfrak{a}\mathfrak{I}_{ij} * (T - 273.15)$$

ij	$\mathfrak{a}\mathfrak{a}_{ij}$	$\mathfrak{a}\mathfrak{I}_{ij}$	$\mathfrak{a}\mathfrak{a}_{ji}$	$\mathfrak{a}\mathfrak{I}_{ji}$	α_{ij}
12	−441.20	18.3280	3,293.17	17.0471	0.475000
13	13,527.42	−92.7391	−4,351.97	53.3769	0.370400
23	1,383.43	8.0409	−1,445.97	−9.1506	0.185894

Ethanol–Water–Methanol System

$\Lambda_{12} = 206.7 \quad \Lambda_{21} = 5{,}270.3 \quad \Lambda_{41} = 0 \quad \alpha_{ij} = 0.4$

$\Lambda_{14} = 0 \quad \Lambda_{24} = 3{,}641.5 \quad \Lambda_{42} = -788.20$

class always give feasible separation at infinite reflux, as shown in the analysis of Laroche et al. (1992b). Ethylene glycol (H) is a heavy entrainer that does not introduce any new azeotropes or residue-curve boundaries, as shown in the residue curve map in Figure 7b, and is classified as case 100. From analysis of the residue-curve map, separation in this case is infeasible at infinite reflux but feasible at finite reflux (see Laroche et al., 1992b). Both these entrainers can facilitate the separation by forming a homogeneous mixture with the feed.

Four synthesis tasks (see Table 5) are considered for an ethanol and water liquid feed of composition $X_A = 0.85$ and $X_B = 0.15$ at a flow rate of 10 kmol/s and conditions of 351.3 K, 1 atm. The NRTL equation was utilized to describe the nonidealities, and the thermodynamic data used are given in Table 4. Pure component enthalpy data are obtained from Daubert and Danner (1985) and Reid et al. (1987). Since the total system pressure is fixed at 1 atm, the behavior of the vapor phase is assumed to be ideal with $\phi_c = 1$. The product

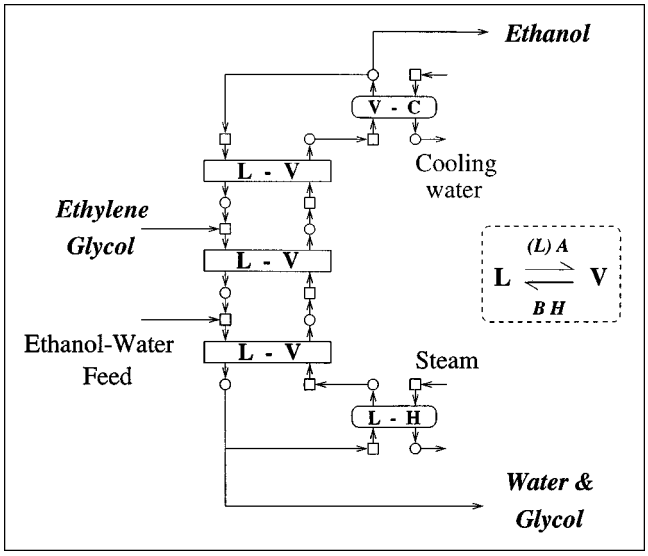

Figure 8. Task 1 results: specifying X prod$_{\text{ethanol}} \geq 0.99$.

specifications for each synthesis task and the results obtained are summarized in Table 5.

Note that for tasks 1 and 2, the synthesis framework identifies the need for an entrainer to break up the azeotrope, as shown in Figures 8 and 9. To achieve a pure ethanol product (see Figure 8, task 1), the ethylene glycol entrainer is chosen to facilitate the separation, which is realized in three $L_{AB}-V_{AB}$ matches, with mass transfer of ethanol from the liquid to the vapor stream. Three mass/heat-exchange modules are interconnected in a configuration that can be recognized as a single extractive column. The ethylene glycol is fed in above the feed (represented by a single module) at a solvent-to-feed ratio of 0.72, increasing the relative volatility of ethanol more than that of water and breaking up the azeotrope to achieve a pure ethanol liquid product that emerges from the cooler. Figure 10 shows the temperature and composition profiles of the extractive column. Note that although the tray-to-tray details are lost, all the main features of an extractive column are captured: (1) maximum temperature in the extractive section due to the greater entrainer concentration in the liquid between the feed trays; (2) the ethanol concentration changes abruptly and approaches zero at the bottom of the column, and there is no ethylene glycol in the distillate product; (3) in the extractive and most of the stripping section the liquid concentration of ethylene glycol is approximately constant, reaching a maximum at the bottom (see Meirelles et al., 1992).

By specifying a high-purity water product in task 2, the light methanol entrainer is selected, which results in the configu-

Table 5. Summary of Separation Tasks for Ethanol–Water Example

	Product Specification	Objective	Entrainer	$F_{\text{entrainer}}$ to F_{feed}	No. Mass/Heat Modules	No. Pure Heat Modules	Utility Cost \$/yr × 10^3
Task 1	$X_{\text{ethanol}} \geq 0.99$	Minimize Cost	Glycol	0.72	4	2	113.1
Task 2	$X_{\text{water}} \geq 0.99$	Minimize Cost	Methanol	7.0	3	2	682.2
Task 3	$X_{\text{ethanol}} \geq 0.99$	Minimize Cost	Glycol	0.72	5	4	159.2
	$X_{\text{water}} \geq 0.99$	$\text{Cost}_{\text{glycol}} \ll \text{Cost}_{\text{methanol}}$					
Task 4	$X_{\text{ethanol}} \geq 0.99$	Minimize Cost	Methanol	7.0	4	4	1433.8
	$X_{\text{water}} \geq 0.99$	$\text{Cost}_{\text{methanol}} \ll \text{Cost}_{\text{glycol}}$					

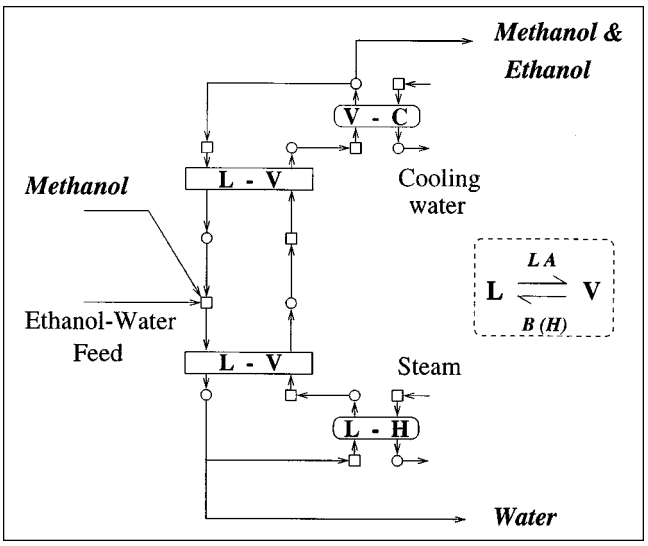

Figure 9. Task 2 results: specifying $X\,\mathrm{prod}_{\mathrm{water}} \geq 0.99$.

ration shown in Figure 9. In this case, two liquid/vapor matches are sufficient to accommodate the separation, whereby methanol facilitates the mass transfer of water from the vapor to the liquid to result in a pure-water product emerging from the bottom of the column. Methanol and ethanol, which have the greater volatility, are transferred from the liquid to the vapor to appear in the distillate. A high solvent-to-feed ratio of 7 is required to achieve the required purity.

Tasks 3 and 4 are concerned with the case of high-purity specifications required on both products. For the case where

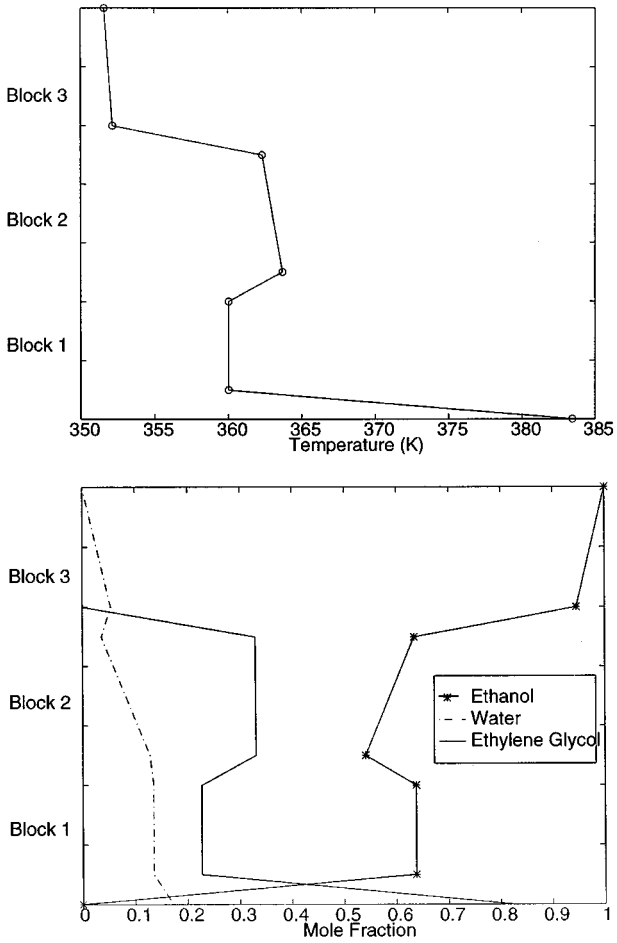

Figure 10. Task 1: temperature–composition profiles.

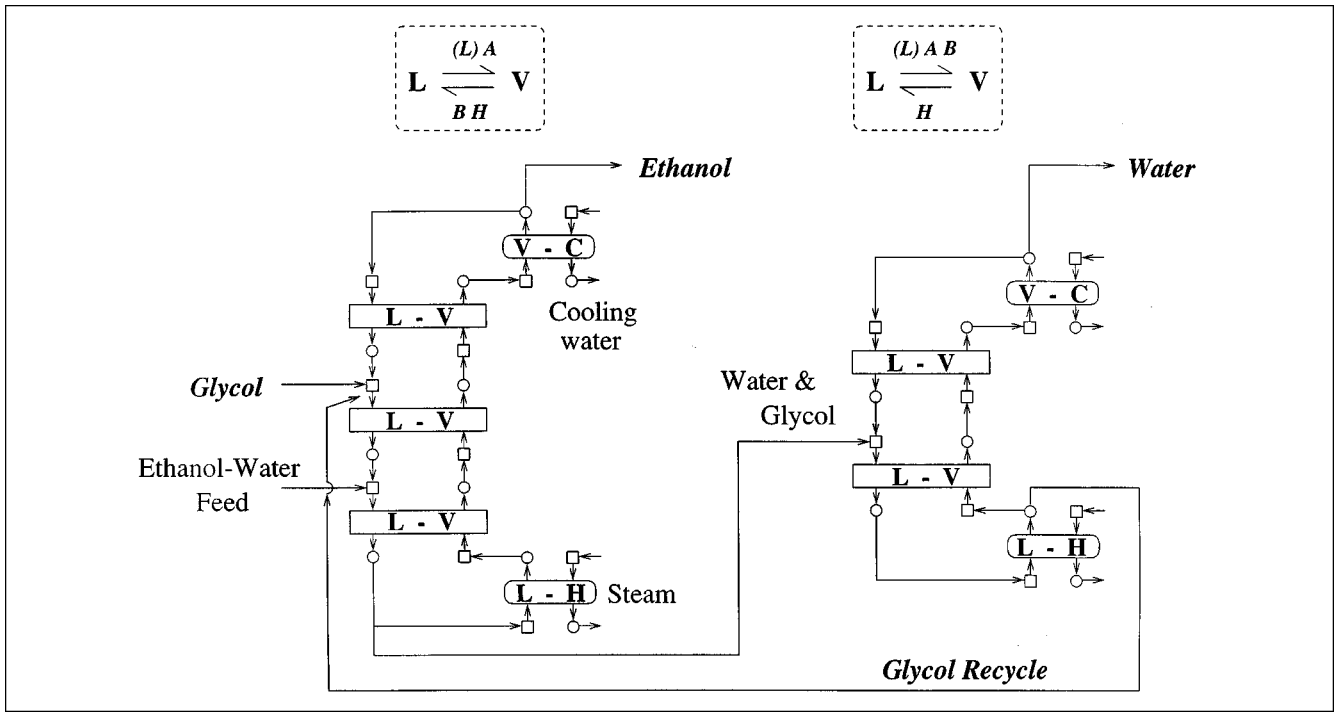

Figure 11. Task 3: results for ethanol–water separation.

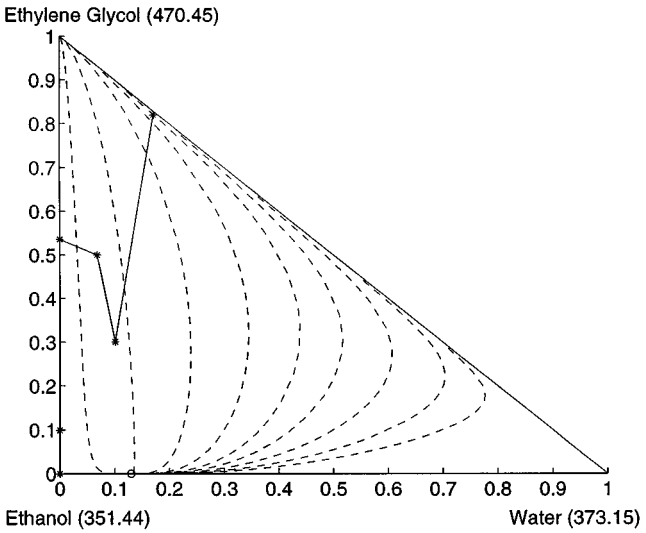

Figure 12. Task 3: composition profile of extractive unit.

the choice of ethylene glycol is more economical, that is, $\text{Cost}_{\text{ethylene glycol}} \ll \text{Cost}_{\text{methanol}}$, the synthesis model results in the configuration, shown in Figure 11, involving five liquid/vapor matches and four pure heat-exchanger matches interconnected. Note that three liquid/vapor matches corresponding to the mass transfer of *ethanol* to the vapor stream (and that of water and ethylene glycol to the liquid stream) represent the extractive column, whose composition profile is shown in Figure 12. Two matches corresponding to mass transfer of *water* to the vapor stream (and that of ethylene glycol to the liquid stream) represent the recovery column. Both the ethanol and water-product streams appear as distillates in this configuration.

For task 4, when $\text{Cost}_{\text{methanol}} \ll \text{Cost}_{\text{ethylene glycol}}$, methanol is selected as the optimal choice in the optimal separation configuration, shown in Figure 13, involving four mass/heat-transfer modules. Two liquid/vapor matches whereby *water* is transferred from the vapor to the liquid stream (with ethanol and methanol transfer to the vapor stream) represents the azeotropic unit. In these matches, the addition of methanol increases the relative volatility between ethanol and water, resulting in a *NA/B* split, with a pure water product appearing as the bottoms. The composition profile for this separator is given in Figure 14. The resulting ethanol and methanol mixture is fed to the next two mass/heat-transfer modules corresponding to a *N/A* split. In these matches, the mass transfer of methanol occurs toward the vapor stream while the liquid stream is enriched in ethanol. The configuration of these matches represents the recovery column whereby a pure ethanol product appears as bottom product and methanol is recycled.

In terms of utility cost, the separation scheme utilizing ethylene glycol as entrainer is more economical than that with methanol, as illustrated in Table 6. In order to achieve the product purity in the azeotropic column with methanol, a high entrainer-to-feed ratio of 7 is required to increase the relative volatility between ethanol and water sufficiently. In addition, the azeotropic column as high reboil ratios with large internal flow rates. These two factors lead to high heating and cooling duties in both the azeotropic and recovery col-

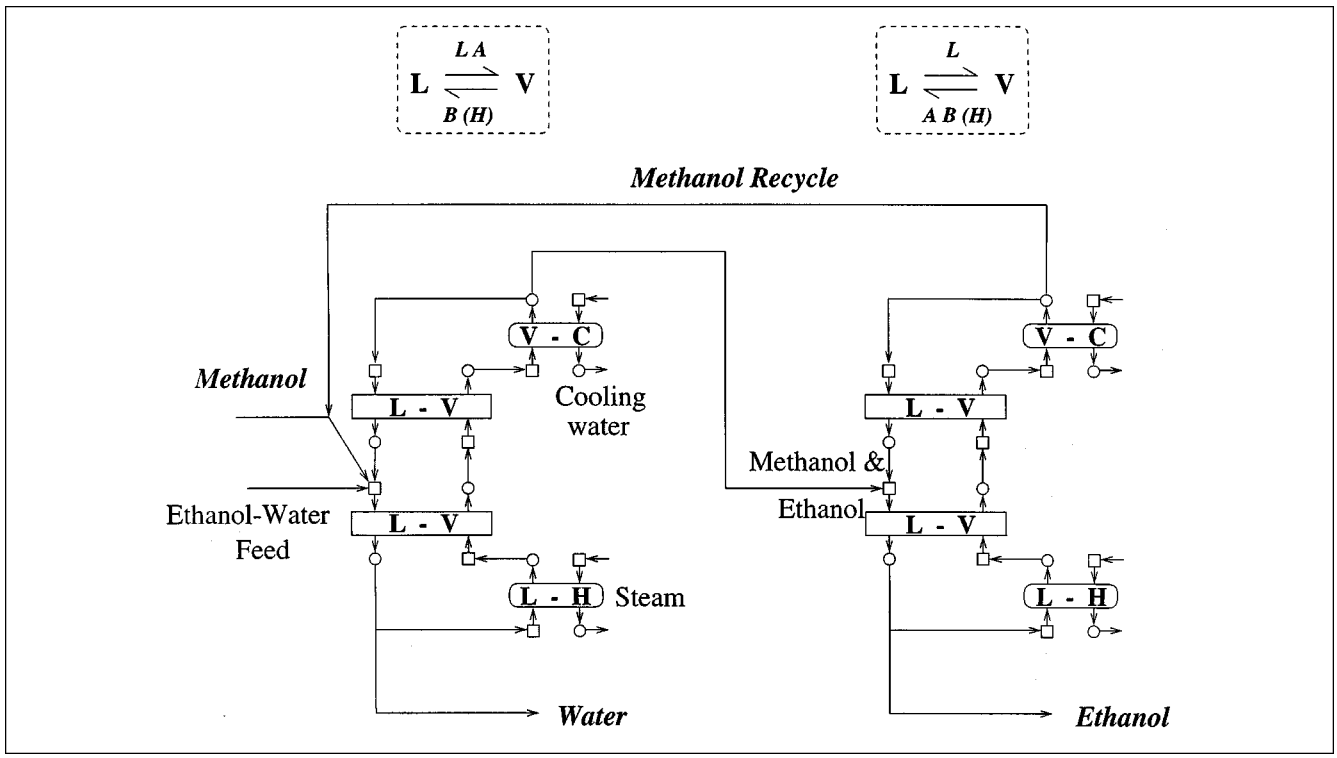

Figure 13. Task 4: results for ethanol–water separation.

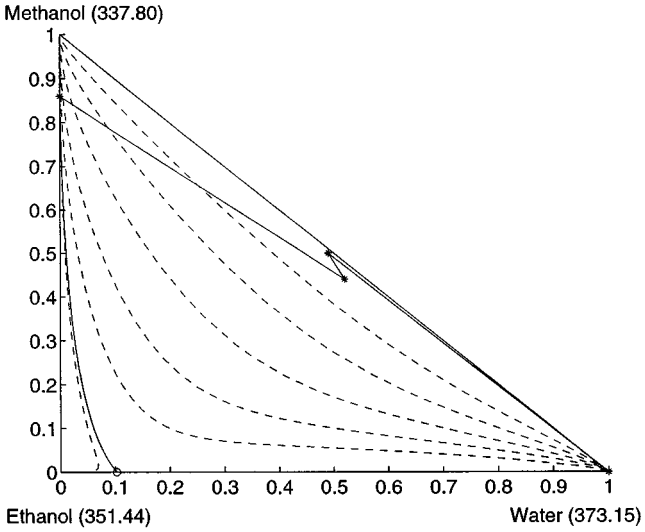

Figure 14. Task 4: composition profile of azeotropic unit.

umn, and thus a high operating cost. In contrast, the extractive column with glycol requires a lower entrainer-to-feed ratio of 0.72 and relatively smaller internal flow rates in both columns (with low reflux and reboil ratios), and thus a lower utility cost.

Example 2: separation of acetone and chloroform

The separation of an acetone (A) and chloroform (C) mixture is considered, given benzene (B) and methanol (M) as available entrainers. Acetone (normal bp of 329.45 K) and chloroform (normal bp 334.35 K) form a maximum boiling azeotrope of 34.5 mol % acetone at a temperature of 337.65 K (1 atm). Benzene introduces no new azeotropes to the system (see Figure 15a), while methanol introduces two new binary azeotropes and a ternary azeotrope, as shown in Figure 15b.

An atmospheric acetone–chloroform liquid feed of composition $X_{\text{acetone}} = 0.60$, $X_{\text{chloroform}} = 0.40$ at a flow rate of 10 kmol/s and a temperature of 330.15 K is considered, with product specifications of a pure liquid acetone and chloroform required. To describe the nonideality in the liquid phase, the Wilson model is used, and the vapor phase is assumed to be ideal. The thermodynamic data used are given in Table 7.

The synthesis model results in the selection of benzene as the optimal entrainer. When the mass/heat-exchange module is heavily penalized in the cost function (indicating an important capital-cost weighting function), the structure shown in Figure 16 is proposed for the separation. Four mass/heat modules are utilized interconnected in a configuration that can be realized as two distillation columns in series. The acetone–chloroform and benzene feed are fed into the liquid mixer of the same mass/heat block. In the first two mass/heat exchangers, acetone is transferred to the vapor phase and chloroform and benzene to the liquid phase. A pure acetone product emerges from this separation "unit." The liquid chloroform and benzene stream are then fed to the next two mass/heat-exchange blocks, where chloroform is transferred to the vapor phase and benzene to the liquid phase. The recovered benzene is recycled to the first separator, and a pure chloroform product appears as the distillate of the second separator. Feasible separation in this system is achieved by crossing the simple distillation boundary, as shown in Figure 17. The cost of crossing the boundary is a

Table 6. Summary of Results for Tasks 3 and 4

	Task 3 Ethylene Glycol		Task 4 Methanol	
$F_{\text{solv}}/F_{\text{feed}}$	0.72		7.0	
T_{solv} (K)	362		337	
Utility Cost \$/yr $\times 10^3$	159.2		1433.8	
	Col. 1	Col. 2	Col. 1	Col. 2
Q_{heating} (kW)	658.9	337.3	3,364.3	5,579.3
Q_{cooling} (kW)	670.9	184.7	3,392.0	4,477.9

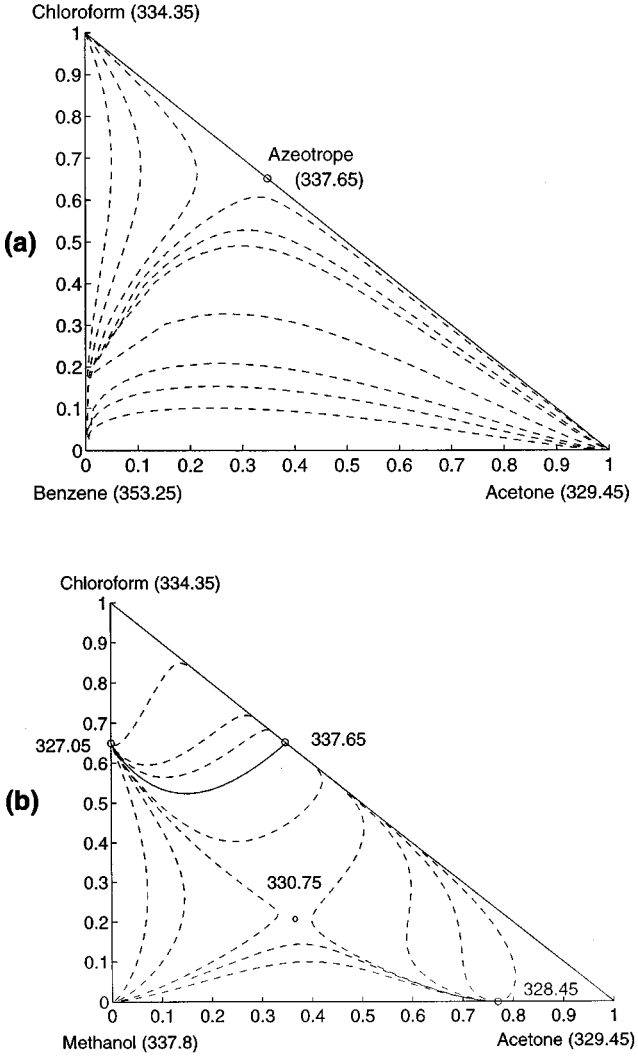

Figure 15. Residue curve maps for acetone–chloroform at 1 atm.

(a) Acetone, chloroform, and benzene mixture. (b) Acetone, chloroform, and methanol mixture.

Table 7. Acetone–Chloroform Separation: Thermodynamic Properties

Component	$C1$	$C2$	$C3$	v_i m^3/mol
Acetone	7.6313	1,566.69	273.419	73.93×10^{-6}
Chloroform	7.44777	1,488.99	264.915	80.662×10^{-6}
Benzene	6.87987	1,196.76	219.161	89.503×10^{-6}
Methanol	7.97010	1,521.23	233.970	40.69×10^{-6}

$$\log P^{sat} = C1 - \frac{C2}{C3+T} \quad \text{(mm Hg, °C)}$$

Wilson Equation

$$\ln\gamma_i = 1 - \ln\left[\sum_j x_j\Lambda_{ij}\right] - \sum_k \frac{x_k\Lambda_{ki}}{\sum_j x_j\Lambda_{kj}}$$

$$\Lambda_{ij} = \frac{v_j}{v_i}\exp\left(\frac{-A_{ij}}{RT}\right) \qquad A_{ii} = 0$$

Binary Interaction Parameters A_{ij} (cal/mol)

	Acetone	Chloroform	Benzene	Methanol
Acetone	0.0	28.8819	543.9352	−161.8813
Chloroform	−484.3856	0.0	−161.8065	−351.1964
Benzene	−182.5230	49.6010	0.0	183.0383
Methanol	583.1054	1,760.6741	1,734.4181	0.0

Data from Gmehling et al. (1979–1988).

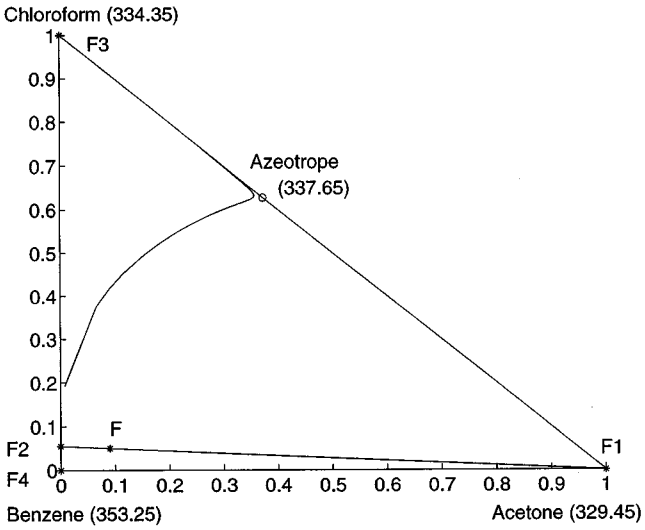

Figure 17. Acetone–chloroform structure 1: liquid composition profile.

high benzene recycle rate and high reboiler duties, as can be seen in Table 8.

When the cost of the mass/heat module is reduced, the synthesis model results in an alternative separation structure, again utilizing benzene as the entrainer. The Six mass/heat-exchange modules shown in Figure 18 are interconnected as in a three-column sequence. In the first two mass/heat blocks, acetone is transferred from the liquid to the vapor stream. Due to a lower ratio of benzene entrainer to fresh feed in this separator, however, not all the acetone emerges as the top product. Some acetone appears with the chloroform and benzene in the bottom liquid product, and the simple distillation boundary is *not* crossed (see the liquid profile of this separation sequence in Figure 19). This liquid is fed to a second separator consisting of two mass/heat modules and two pure heat blocks, where acetone and chloroform are transferred to the vapor stream and the benzene to the liquid stream. In this unit, pure liquid benzene is obtained as the bottom product and recycled to the first ''unit.'' The top product of this separator (F3) is on the chloroform side of the azeotrope (Figure 19) and is fed to the next two mass/heat exchangers. In these blocks chloroform is transferred to the vapor phase, resulting in the desired pure chloroform stream,

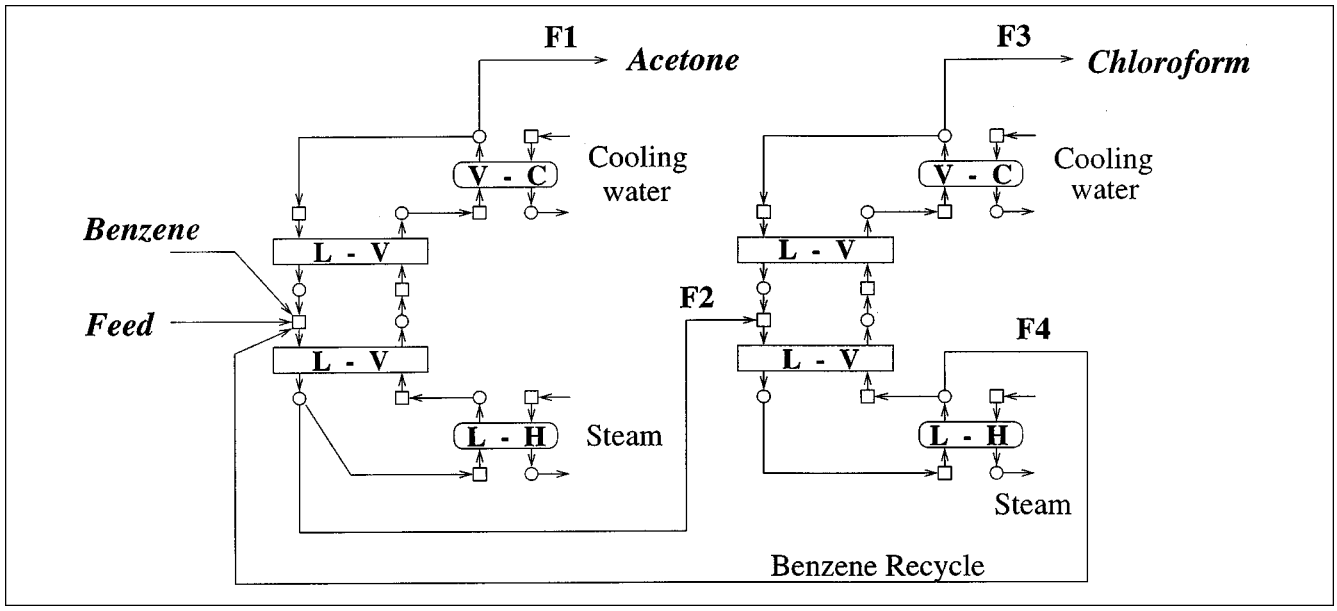

Figure 16. Acetone–chloroform: structure 1.

Table 8. Acetone–Chloroform Structure 1

Stream	Total Flow (kmol/s)	Component Molar Flows			Temp. (K)
		Acetone	Chloroform	Benzene	
Feed	10.0000	6.0000	4.0000	0.0000	330.15
Makeup	0.0030	0.0000	0.0000	0.0030	353.30
F1	6.0026	5.9601	0.0396	0.0029	329.30
F2	60.8014	0.0399	3.9604	56.8011	352.80
F3	4.0004	0.0399	3.9604	0.0001	334.10
F4	56.8010	0.0000	0.0000	56.8010	353.30
		$Q_{\text{heating},1}$	2,843.49 kW		
		$Q_{\text{heating},2}$	2,660.79 kW		
		$Q_{\text{heating},T}$	5,504.28 kW		

but the amount of mass transfer allowed is limited by the azeotropic composition that emerges as the bottom product. This stream (F6) is recycled to the first separator.

It is interesting to note how the trade-offs between capital and operating cost can be captured within the proposed synthesis framework, even when the exact capital cost functions cannot be employed. In the first case, when a high ''capital cost'' is considered for each mass/heat-exchange module, the separation is achieved in a small number of modules (that can correspond to two separation units). In order to cross the distillation boundary, however, a high benzene recycle is required, and thus high heating duties (see Table 9). When heating is reduced, the distillation boundary is not crossed and high-purity chloroform is obtained at the cost of two extra mass/heat-exchange modules (that is, an extra separator). Furthermore, the ''three column'' sequence has better operational characteristics, and is not subject to the uncertainty of boundary crossing in the two-column sequence (due to the sensitivity of the design to the parameters in the thermodynamic model). Detailed design issues can be studied in the second stage for the proposed alternatives to evaluate the actual cost requirements.

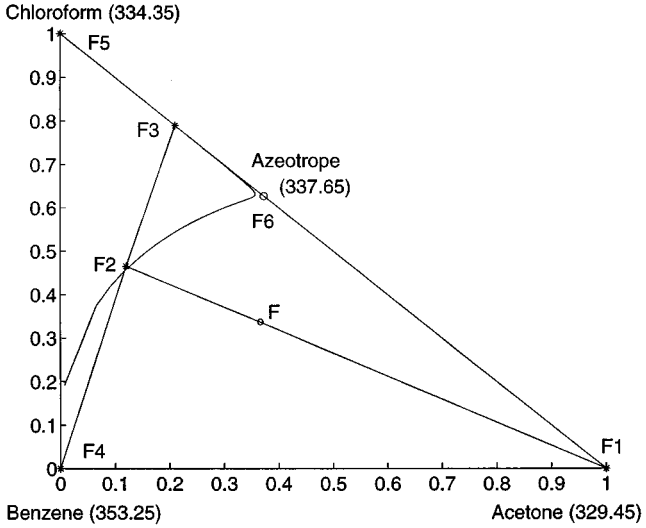

Figure 19. Acetone–chloroform structure 2: liquid composition profile.

Concluding Remarks

A mass/heat-exchange superstructure modular representation for synthesizing homogeneous azeotropic separation systems has been proposed in this work. The model features (1) generic expressions for the consistent determination of the mass-transfer direction within the optimization procedure,

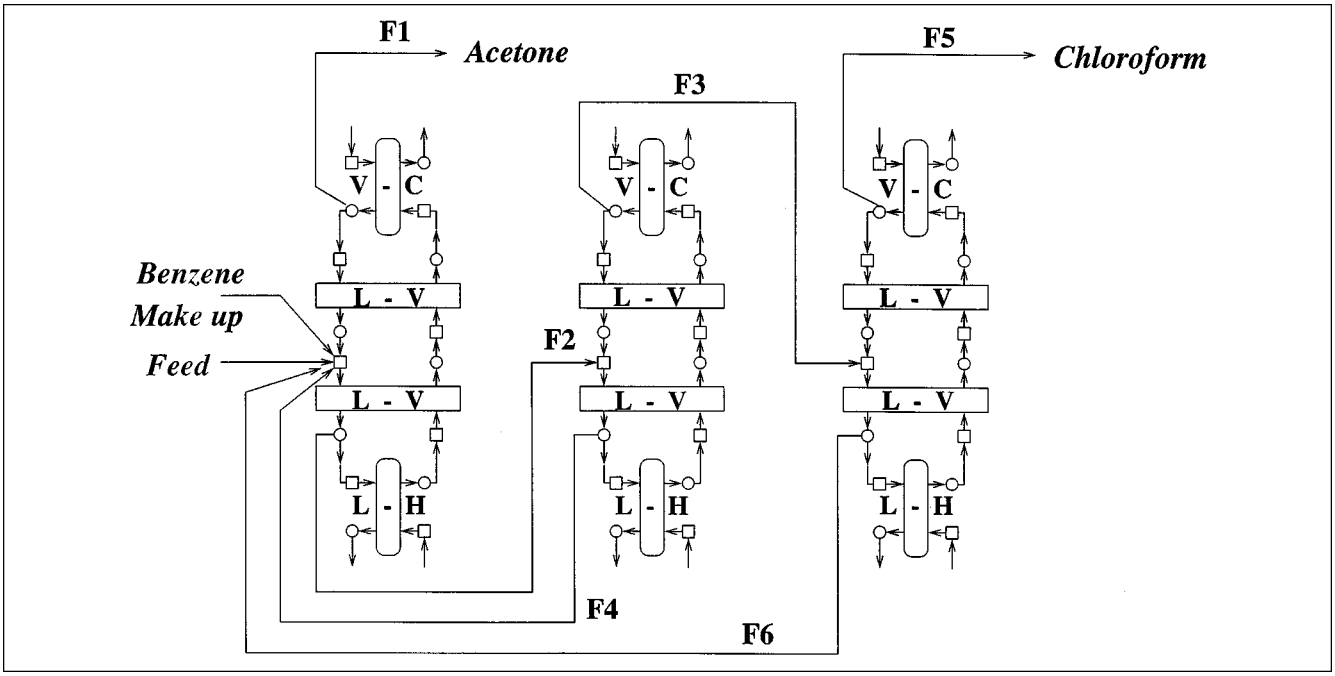

Figure 18. Acetone–chloroform: structure 2.

Table 9. Acetone–Chloroform Structure 2

Stream	Total Flow (kmol/s)	Composition $X_{Acetone}$	$X_{Chloroform}$	$X_{Benzene}$	Temp. (K)
Feed	10.000	0.600	0.400	0.000	330.15
F1	6.000	1.000	0.000	0.000	
F2	16.220	0.120	0.465	0.415	352.8
F3	9.550	0.210	0.790	0.000	
F4	6.670	0.000	0.000	1.000	353.3
F5	3.999	0.000	1.000	0.000	
F6	5.550	0.360	0.640	0.000	338.0

$Q_{heating,1}$	1,459.80 kW
$Q_{heating,2}$	2,059.70 kW
$Q_{heating,3}$	1,030.08 kW
$Q_{heating,T}$	4,549.58 kW

and (2) multipurpose mass/heat-exchange modules, through the combinations of which separation units and structures can be realized. Since each mass/heat-transfer module corresponds to a certain mass-transfer pattern, the final structure obtained usually consists of a small number of modules, each of which represents a whole or a part of a separation unit. As illustrated by two representative separation example problems, the proposed representation and synthesis methodology can potentially identify the promising separation schemes (that is, columns), their sequence, and required entrainers, simultaneously without any prepostulation of units. Feasible alternatives optimal with respect to an economic objective function are achieved, and can be utilized as a starting point for a more detailed design.

Acknowledgments

Financial support from the European Communities, under contract JOE3-CT95-0017 (IDEES project), is gratefully acknowledged. The authors also acknowledge the useful comments provided by Professor W. D. Seider on an earlier draft of the article.

Notation

K_c = vapor/liquid equilibrium constant of component c
n_c = component number of moles
$(nG)^{tot}$ = total Gibbs free energy
P_c^{sat} = saturated vapor pressure of component c
P_{tot} = system pressure
R = gas constant
S = entropy
$\mathbb{V}$ = volume
x_c = molar fraction of component c
ΔG_c^f = standard Gibbs free energy of formation
μ_c = chemical potential of component c

Superscripts and subscript

s = superstructure stream
LI = liquid inlet stream
LO = liquid outlet stream
VI = vapor inlet stream
VO = vapor outlet stream
c = component

Literature Cited

Bauer, M. H., and J. Stichlmair, "Synthesis and Optimization of Distillation Sequences for the Separation of Azeotropic Mixtures," *Comput. Chem. Eng.*, **19**, S15 (1995).

Bekiaris, N., and M. Morari, "Multiple Steady-States in Distillation —Infinity/Infinity Predictions, Extensions, and Implications for Design, Synthesis and Simulation," *Ind. Eng. Chem. Res.*, **35**, 4264 (1996).

Biegler, L. T., I. E. Grossmann, and A. W. Westerberg, *Systematic Methods of Chemical Process Design*, Chap. 14, Prentice Hall, Englewood Cliffs, NJ (1997).

Brooke, A., D. Kendrick, and A. Meeraus, *GAMS: A User Guide*, The Scientific Press, San Francisco (1988).

Castillo, F. J. L., D. Y. C. Thong, and G. P. Towler, "Homogeneous Azeotropic Distillation: 1. Design Procedure for Single-Feed Columns at Nontotal Reflux," *Ind. Eng. Chem. Res.*, **37**, 987 (1998).

Daubert, T. E., and R. P. Danner, *Data Compilation Tables of Properties of Pure Components*, Design Institute for Physical Property Data, AIChE, New York (1985).

Doherty, M. F., and G. A. Caldarola, "Design and Synthesis of Homogeneous Azeotropic Distillations: 3. Sequencing of Columns for Azeotropic and Extractive Distillations," *Ind. Eng. Chem. Fundam.*, **24**, 474 (1985).

Fidkowski, Z. T., M. F. Doherty, and M. Malone, "Feasibility of Separations for Distillation of Nonideal Ternary Mixtures," *AIChE J.*, **39**, 1303 (1993).

Foucher, E. R., M. F. Doherty, and M. F. Malone, "Automatic Screening of Entrainers for Homogeneous Azeotropic Distillation," *Ind. Eng. Chem. Res.*, **30**, 760 (1991).

Gmehling, J., U. Onken, and W. Arlt, *Vapor-Liquid Equilibrium Data Collection*, Chemistry Data Series, Vol. I/3 + 4, DECHEMA, Frankfurt (1979).

Gmehling, J., U. Onken, and W. Arlt, *Vapor-Liquid Equilibrium Data Collection*, Chemistry Data Series, Vol. I/7, DECHEMA, Frankfurt (1980).

Gmehling, J., U. Onken, and W. Arlt, *Vapor-Liquid Equilibrium Data Collection*, Chemistry Data Series, Vol. I/2e, DECHEMA, Frankfurt (1988).

Jobson, M., D. Hilderbrandt, and D. Glasser, "Attainable Products for the Vapor-Liquid Separation of Homogeneous Ternary Mixtures," *Chem. Eng. J. & Bio. Eng. J.*, **59**, 51 (1995).

Julka, V., and M. F. Doherty, "Geometric Behavior and Minimum Flows for Nonideal Multicomponent Distillation," *Chem. Eng. Sci.*, **45**, 1801 (1990).

Knapp, J. P., and M. F. Doherty, "Minimum Entrainer Flows for Extractive Distillation: A Bifurcation Theoretical Approach," *AIChE J.*, **40**, 243 (1994).

Knight, J. R., and M. F. Doherty, "Design and Synthesis of Homogeneous Azeotropic Distillations: 5. Columns with Non-Negligible Heat Effects," *Ind. Eng. Chem. Fundam.*, **25**, 279 (1986).

Laroche, L., N. Bekiaris, H. W. Andersen, and M. Morari, "Homogeneous Azeotropic Distillation: Comparing Entrainers," *Can. J. Chem. Eng.*, **69**, 1302 (1991).

Laroche, L., N. Bekiaris, H. W. Andersen, and M. Morari, "The Curious Behaviour of Homogeneous Azeotropic Distillation-Implications for Entrainer Selection," *AIChE J.*, **38**, 1309 (1992a).

Laroche, L., N. Bekiaris, H. W. Andersen, and M. Morari, "Homogeneous Azeotropic Distillation: Separability and Flowsheet Synthesis," *Ind. Eng. Chem. Res.*, **31**, 2190 (1992b).

Levy, S. G., D. B. Van Dongen, and M. F. Doherty, "Design and Synthesis of Homogeneous Azeotropic Distillation: 2. Minimum Reflux Calculations for Nonideal and Azeotropic Columns," *Ind. Eng. Chem. Fundam.*, **24**, 463 (1985).

Malone, M. F., and M. F. Doherty, "Separation System Synthesis for Nonideal Liquid Mixtures," FOCAPD Conf., Snowmass, CO (1994).

Meirelles, A., S. Weiss, and H. Herfurth, "Ethanol Dehydration by Extractive Distillation," *J. Chem. Tech. Biotechnol.*, **53**, 181 (1992).

Papalexandri, K. P., and E. N. Pistikopoulos, "Generalized Modular Representation Framework for Process Synthesis," *AIChE J.*, **42**, 1010 (1996).

Reid, R. C., J. M. Prausnitz, and B. E. Poling, *The Properties of Gases and Liquids*, 4th ed., McGraw-Hill, New York (1987).

Rooks, R. E., V. Julka, M. F. Doherty, and M. F. Malone, "Structure of Distillation Regions for Multicomponent Azeotropic Mixtures," *AIChE J.*, **44**, 1382 (1998).

Safrit, B. T., and A. W. Westerberg, "Algorithm for Generating the Distillation Regions for Azeotropic Multicomponent Mixtures," *Ind. Eng. Chem. Res.*, **36**, 1827 (1997a).

Safrit, B. T., and A. W. Westerberg, ''Synthesis of Azeotropic Batch Distillation Separation Systems,'' *Ind. Eng. Chem. Res.*, **36**, 1841 (1997b).
Smith, J. M., and H. C. Van Ness, *Introduction to Chemical Engineering Thermodynamics*, 4th ed., McGraw-Hill, Singapore (1987).
Stichlmair, J., J. F. Fair, and J. L. Bravo, ''Separation of Azeotropic Mixtures via Enhanced Distillation,'' *Chem. Eng. Prog.*, **85**, 63 (1989).
Stichlmair, J., and J. Herguijuela, ''Separation Regions and Processes of Zeotropic and Azeotropic Ternary Distillation,'' *AIChE J.*, **38**, 1523 (1992).
Stichlmair, J. G., H. Offers, and R. W. Potthoff, ''Minimum Reflux and Minimum Reboil in Ternary Distillation,'' *Ind. Eng. Chem. Res.*, **32**, 2438 (1993).
Wahnschafft, O. M., T. P. Julian, and A. W. Westerberg, ''SPLIT: A Separation Process Designer,'' *Comput. Chem. Eng.*, **15**, 565 (1991).
Wahnschafft, O. M., J. W. Koehler, E. Blass, and A. W. Westerberg, ''The Product Composition Regions of Single-Feed Azeotropic Distillation Columns,'' *Ind. Eng. Chem. Res.*, **31**, 2345 (1992a).
Wahnschafft, O. M., J. P. L. Rudulier, P. Blania, and A. W. Westerberg, ''SPLIT: II. Automated Synthesis of Hybrid Liquid Separation Systems,'' *Comput. Chem. Eng.*, **16**, 305 (1992b).
Wahnschafft, O. M., and A. W. Westerberg, ''The Product Composition Regions of Azeotropic Distillation Columns: II. Separability in Two-Feed Columns and Entrainer Selection,'' *Ind. Eng. Chem. Res.*, **32**, 1108 (1993).
Westerberg, A. W., and O. Wahnschafft, ''Synthesis of Distillation-Based Separation Processes,'' *Advances in Chemical Engineering*, Vol. 23, Process Synthesis, J. P. Anderson, ed., Academic Press, New York, p. 63 (1996).
Widagdo, S., and W. D. Seider, ''Azeotropic Distillation,'' *AIChE J.*, **42**, 96 (1996).

Appendix A: Mass-Transfer Driving-Force Constraints

Consider a multicomponent liquid/vapor mixture. For the total Gibbs free energy, we have (Smith and Van Ness, 1987)

$$d(nG)^{\text{tot}} = (n\mathcal{V})\,dP - (nS)\,dT + \sum_c \left(\mu_c^L\, dn_c^L + \mu_c^V\, dn_c^V\right), \tag{A1}$$

where superscripts L and V denote the liquid and vapor phases, respectively.

Since no reaction takes place, mass conservation for each component c requires

$$n_c^L + n_c^V = \text{constant}$$

and

$$dn_c^L + dn_c^V = 0.$$

Thus at constant temperature T and pressure P,

$$d(nG)^{\text{tot}} = \sum_{c=1}^{C} \left(\mu_c^L - \mu_c^V\right) dn_c^L. \tag{A2}$$

At constant T and P, a component c is transferred from the liquid to the vapor phase when both the Gibbs free energy of the system decreases $d(nG)^{\text{tot}} \le 0$ and the liquid holdup of c decreases $dn_c^L \le 0$, that is,

$$\frac{\partial (nG)^{\text{tot}}}{\partial n_c^L} = \mu_c^L - \mu_c^V \ge 0. \tag{A3}$$

Similarly, for mass transfer of c from the vapor to the liquid,

$$\frac{\partial (nG)^{\text{tot}}}{\partial n_c^L} = \mu_c^L - \mu_c^V \le 0. \tag{A4}$$

The chemical potential of the liquid and vapor streams are given by

$$\mu_c^L = \Delta G_c^{f,L} + RT \ln\left(\gamma_c x_c^L\right)$$
$$\mu_c^V = \Delta G_c^{f,V} + RT \ln\left(\phi_c x_c^V P_{\text{tot}}\right).$$

Assuming a negligible effect of pressure on $\Delta G_c^{f,L}$

$$\Delta G_c^{f,L} \approx \Delta G_c^{f,V} + RT \ln\left(P_c^{\text{sat}}\right). \tag{A5}$$

From Eq. A3, transfer from liquid to vapor occurs when

$$\Delta G_c^{f,V} + RT \ln\left(P_c^{\text{sat}}\right) + RT \ln\left(x_c^L \gamma_c\right) \ge \Delta G_c^{f,V} + RT \ln\left(\phi_c x_c^V P_{\text{tot}}\right)$$

$$\leftrightarrow \ln\left(\frac{\gamma_c P_c^{\text{sat}}}{\phi_c P_{\text{tot}}} x_c^L\right) \ge \ln\left(x_c^V\right)$$

$$\leftrightarrow \frac{\gamma_c P_c^{\text{sat}}}{\phi_c P_{\text{tot}}} x_c^L \ge x_c^V$$

$$\leftrightarrow K_c x_c^L \ge x_c^V, \quad \text{where} \quad K_c = \frac{\gamma_c P_c^{\text{sat}}}{\phi_c P_{\text{tot}}}. \tag{A6}$$

Similarly, for mass transfer from the vapor to liquid,

$$K_c x_c^L \le x_c^V \tag{A7}$$

must hold.

Appendix B: Mass/Heat-Exchange Superstructure Model

Consider the mass/heat exchange-module of Figure 2b and the reduced mass/heat-exchange superstructure as described in the section titled ''Mass/heat-exchange network superstructure model.'' The existence (or not) of each module in the final flow sheet is denoted by a binary variable

$$y_e = \begin{cases} 1, & \text{if module } e \text{ exists} \\ 0, & \text{otherwise.} \end{cases}$$

Considering liquid feeds and products, the following sets are introduced for the streams of the mass/heat-exchange

superstructure:

I = {n/n initial stream including given feeds and possible entrainers}
P = {p/p product stream}
LI_e = {s/s liquid inlet stream li in mass/heat exchanger e}
LO_e = {s/s liquid outlet stream lo in exchanger e}
VI_e = {s/s vapor inlet stream vi in mass/heat exchanger e}
VO_e = {s/s vapor outlet stream vo in exchanger e}
HI_e = {s/s inlet stream hi of the utility heater of module e}
HO_e = {s/s outlet stream ho of the utility heater of module e}
CI_e = {s/s inlet stream ci of the utility cooler of module e}
CO_e = {s/s outlet stream co of the utility cooler of module e}
$LL_{ee'}$ = {s/s interconnecting stream from liquid outlet splitter of module e to liquid inlet mixer of module e'}
$VV_{ee'}$ = {s/s interconnecting stream from vapor outlet splitter of module e to vapor inlet mixer of module e'}
$LH_{ee'}$ = {s/s interconnecting stream from liquid outlet splitter of module e to utility heater of module e'}
$HV_{ee'}$ = {s/s interconnecting stream from utility heater to module e to vapor inlet mixer of module e'}
$VC_{ee'}$ = {s/s interconnecting stream from vapor outlet splitter of module e to utility cooler of module e'}
$CL_{ee'}$ = {s/s interconnecting stream from utility cooler of module e to liquid inlet mixer of module e'}
IL_{ne} = {s/s interconnecting stream from initial stream n to liquid inlet mixer of module e}
IH_{ne} = {s/s interconnecting stream from initial stream n to utility heater of module e}
IP_{np} = {s/s interconnecting stream from initial stream n to final mixer of product p}
LP_{ep} = {s/s interconnecting stream from liquid outlet splitter of module e to final mixer of product p}
CP_{ep} = {s/s interconnecting stream from utility cooler of module e to final mixer of product p}

$$\mathbb{S} = I \cup P \cup LI_e \cup LO_e \cup VI_e \cup VO_e \cup HI_e \cup HO_e \cup CI_e \cup CO_e \cup LL_{ee'} \cup VV_{ee'} \cup LH_{ee'} \cup HV_{ee'} \cup VC_{ee'} \cup CL_{ee'} \cup IL_{ne} \cup IH_{ne} \cup IP_{np} \cup LP_{ep} \cup CP_{ep}$$

$$\mathbb{S}1(\mathbb{S}) = I \cup P \cup LI_e \cup LO_e \cup VI_e \cup VO_e \cup HI_e \cup HO_e \cup CI_e \cup CO_e.$$

The set of initial streams is made up of a set of given feed streams and possible entrainers

$$I = I1 \cup I2$$

$$I1 = \{n1/n1 \text{ set of initial existing feeds}\}$$

$$I2 = \{n2/n2 \text{ set of possible entrainers}\}.$$

The following set of continuous variables are introduced to describe the superstructure streams:

f^s	molar stream flow	$s \in \mathbb{S}$
x_c^s	molar fraction of component c in stream s	
h^s	enthalpy	$s \in \mathbb{S}1$
T^s	temperature	

Since the composition, temperature, and enthalpy of streams coming out of the superstructure splitters are equal to the composition, temperature, and enthalpy of the stream entering the mixer, these variables are only defined for the liquid and vapor inlet and outlet streams of the mass/heat-exchange modules, the inlet and outlet streams of the utility heat exchangers, and the initial and final product streams (subset $\mathbb{S}1$). In addition, since no mass transfer occurs in the utility heat exchangers, the inlet and outlet stream flows and composition through them are unchanged and are described by one set of flow and compositions variables, that is, for the utility cooler, $f^C = f^{CI} = f^{CO}$ and $x_c^C = x_c^{CI} = x_c^{CO}$, for utility heater $f^H = f^{HI} = f^{HO}$ and $x_c^H = x_c^{HI} = x_c^{HO}$. Finally, variable heat loads of the utility exchanger (Qh_e, Qc_e) are defined, positive for heat input, and negative for heat removal. As described in Table 2, binary variables are defined to denote the existence (or not) of superstructure streams in the final flow sheet. Note that these variables are not necessary; thus, their presence does not increase the combinatorial complexity of the synthesis problem. They are utilized to simplify the solution of the nonlinear part of the superstructure model and to facilitate the introduction of logical constraints to the model.

Similarly, the utilization (or not) of an entrainer is denoted by a binary variable

$$y\,\text{solv}_n = \begin{cases} 1, & \text{if entrainer } n \text{ is utilized} \\ 0, & \text{otherwise.} \end{cases}$$

Mass-transfer direction for each component in each module is denoted by a binary variable

$$yt_{ec} = \begin{cases} 1, & \text{when component } i \text{ is transferred from liquid to vapor in module } e \\ 0, & \text{otherwise.} \end{cases}$$

Once again, this variable is not necessary. However, its inclusion simplifies the mass-transfer driving-force constraints.

The mass/heat-exchange superstructure model involves the following elements.

1. Mass balance for total stream flows at

- Initial stream splitters $n \in I$

$$f_n^I - \sum_e f_{ne}^{IL} - \sum_e f_{ne}^{IH} - \sum_p f_{np}^{IP} = 0. \qquad \text{(B1)}$$

- Splitters at the outlets of each side of module e

$$f_e^{LO} - \sum_{e'} \left(f_{ee'}^{LL} + f_{ee'}^{LH} \right) - \sum_p f_{ep}^{LP} = 0 \qquad \text{(B2)}$$

$$f_e^{VO} - \sum_{e^7} \left(f_{ee'}^{VV} + f_{ee'}^{VC} \right) = 0 \qquad \text{(B3)}$$

$$f_e^H - \sum_{e'} f_{ee'}^{HV} = 0 \qquad \text{(B4)}$$

$$f_e^C - \sum_{e'} f_{ee'}^{CL} - \sum_p f_{ep}^{CP} = 0. \qquad \text{(B5)}$$

- Mixers at the inlets of the mass/heat-exchange module e

$$f_e^{LI} - \sum_n f_{ne}^{IL} - \sum_{e'} \left(f_{e'e}^{LL} + f_{e'e}^{CL} \right) = 0 \qquad \text{(B6)}$$

$$f_e^{VI} - \sum_{e'} \left(f_{e'e}^{VV} + f_{e'e}^{HV} \right) = 0. \qquad \text{(B7)}$$

- Mixers of the utility exchangers e

$$f_e^C - \sum_{e'} f_{e'e}^{VC} = 0 \tag{B8}$$

$$f_e^H - \sum_{n} f_{ne}^{IH} - \sum_{e'} f_{e'e}^{LH} = 0. \tag{B9}$$

- Final stream mixers $p \in P$

$$f_p^P - \sum_{n} f_{np}^{IP} - \sum_{e} f_{ep}^{LP} - \sum_{e} f_{ep}^{CP} = 0. \tag{B10}$$

2. Mass balances for each component at

- Mixers prior to the liquid and vapor sides of each module e

$$f_e^{LI} x_{ec}^{LI} - \sum_{n} f_{ne}^{IL} x_{ni}^{I} - \sum_{e'} \left(f_{e'e}^{LL} x_{e'i}^{LO} + f_{e'e}^{CL} x_{e'i}^{C} \right) = 0 \tag{B11}$$

$$f_e^{VI} x_{ec}^{Vi} - \sum_{e'} \left(f_{e'e}^{VV} x_{e'i}^{VO} + f_{e'e}^{HV} x_{e'i}^{H} \right) = 0. \tag{B12}$$

- Mixers prior to the utility exchangers e

$$f_e^C x_{ec}^C - \sum_{e'} f_{e'e}^{VC} x_{e'i}^{VO} = 0 \tag{B13}$$

$$f_e^H x_{ec}^H - \sum_{n} f_{ne}^{IH} x_{ni}^{I} - \sum_{e'} f_{e'e}^{LH} x_{e'i}^{LO} = 0. \tag{B14}$$

- Final mixer of each product stream $p \in P$

$$f_p^P x_c^P - \sum_{n} f_{np}^{IP} x_{ni}^{I} - \sum_{e} \left(f_{ep}^{LP} x_{ec}^{LO} + f_{ep}^{CP} x_{ec}^{C} \right) = 0. \tag{B15}$$

- Around each mass/heat-exchange block

$$f_e^{LI} x_{ec}^{LI} + f_e^{VI} x_{ec}^{VI} - f_e^{LO} x_{ec}^{LO} - f_e^{VO} x_{ec}^{VO} = 0. \tag{B16}$$

3. Energy balances at

- Mixers prior to the liquid and vapor sides of each module e

$$f_e^{LI} h_e^{LI} - \sum_{n} f_{ne}^{IL} h_n^{I} - \sum_{e'} \left(f_{e'e}^{LL} h_{e'}^{LO} + f_{e'e}^{CL} h_{e'}^{CO} \right) = 0 \tag{B17}$$

$$f_e^{VI} h_e^{VI} - \sum_{e'} \left(f_{e'e}^{VV} h_{e'}^{VO} + f_{e'e}^{HV} h_{e'}^{HO} \right) = 0. \tag{B18}$$

- Mixers prior to utility exchangers e

$$f_e^C h_e^{CI} - \sum_{e'} f_{e'e}^{VC} h_{e'}^{VO} = 0 \tag{B19}$$

$$f_e^H h_e^{HI} - \sum_{n} f_{ne}^{IH} h_n^{I} - \sum_{e'} f_{e'e}^{LH} h_{e'}^{LO} = 0. \tag{B20}$$

- Utility exchangers of each module e

$$Qh_e - f_e^H \left(h_e^{HO} - h_e^{HI} \right) = 0 \tag{B21}$$

$$Qc_e - f_e^C \left(h_e^{CO} - h_e^{CI} \right) = 0. \tag{B22}$$

- Around each mass/heat-exchange block e

$$f_e^{LI} h_e^{LI} + f_e^{VI} h_e^{VI} - f_e^{LO} h_e^{LO} - f_e^{VO} h_e^{VO} = 0. \tag{B23}$$

- Final mixers of each product stream $p \in P$

$$f_p^P h^P - \sum_{n} f_{np}^{IP} h_n^{I} - \sum_{e} \left(f_{ep}^{LP} h_e^{LO} + f_{ep}^{CP} h_e^{CO} \right) = 0. \tag{B24}$$

4. Summation of molar fractions: For superstructure streams $s \in \mathfrak{S}1$

$$\sum_{i} x_c^s - 1 = 0. \tag{B25}$$

5. Phase-defining constraints

$$\text{for liquid streams:} \quad \mathfrak{L}\,\mathfrak{G} \le \sum_{c} K_c^s x_c^s \le 1 \quad s \in \mathfrak{S}1 \tag{B26}$$

$$\text{for vapor streams:} \quad \mathfrak{L}\,\mathfrak{G} \le \sum_{c} x_c^s / K_c^s \le 1 \quad s \in S1, \tag{B27}$$

where $\mathfrak{L}\,\mathfrak{G}$ limits the level of superheating and supercooling ($\mathfrak{L}\,\mathfrak{G} = 0.8$ is utilized) and

$$K_c^s = \frac{\gamma_c^s P_c^{\text{sat},s}}{P_{\text{tot}}}. \tag{B28}$$

6. Mass-transfer driving-force constraints for each component: The constraints (Eqs. 3) are rewritten as follows:

$$\left[(y_e - 1) + (yt_{ec} - 1) \right] \mathfrak{U} \le f_e^{LI} x_{ec}^{LI} - f_e^{LO} x_{ec}^{LO} \le yt_{ec} \mathfrak{U} + (1 - y_e) \mathfrak{U} \tag{B29}$$

$$\left[(y_e - 1) + (yt_{ec} - 1) \right] \mathfrak{U} \le K_{ec}^{LI} x_{ec}^{LI} - x_{ec}^{VO} \le yt_{ec} \mathfrak{U} + (1 - y_e) \mathfrak{U} \tag{B30}$$

$$\left[(y_e - 1) + (yt_{ec} - 1) \right] \mathfrak{U} \le K_{ec}^{LO} x_{ec}^{LO} - x_{ec}^{VI} \le yt_{ec} \mathfrak{U} + (1 - y_e) \mathfrak{U}, \tag{B31}$$

where $\mathfrak{U}$ is a (large) positive number and set to the upper bound of mass transfer within the module, usually 10 times the feed rate. We impose without any loss of generality

$$yt_{ec} + y_e \ge 1 \tag{B32}$$

such that in a nonexisting module, all components are transferred from the liquid to the vapor, making the driving force constraints just listed redundant.

7. Thermodynamic property calculation: Stream properties are calculated as a function of their temperature and composition. Any thermodynamic model can be utilized to determine the enthalpy, activity coefficient, and vapor pressure (stream equilibrium constant). Note that in this work constant total system pressure is assumed. If this is not the case, a variable pressure is also assigned to each stream.

8. Process constraints and specifications on desired products: For example, given minimum specifications on product flows and purities $F\,\mathrm{spec}^P$, $X\,\mathrm{spec}_c^P$

$$f^P \geq F\,\mathrm{spec}^P$$

$$x_c^P \geq X\,\mathrm{spec}_c^P.$$

9. Logical constraints

• To define the existence of each module of each superstructure stream

$$\left[f_e^{LI} + f_e^{LO} + f_e^{VI} + f_e^{VO}\right] - y_e \mathfrak{F}^{\max} \leq 0 \qquad \text{(B33)}$$

$$Qh_e - yh_e \mathfrak{Q}^{\max} \leq 0 \qquad \text{(B34)}$$

$$Qc_e - yc_e \mathfrak{Q}^{\max} \leq 0, \qquad \text{(B35)}$$

where $\mathfrak{F}^{\max}$ is an upper bound to stream flows and $\mathfrak{Q}^{\max}$ is an upper bound to heat flows.

• To define the existence of interconnecting streams

$$f_{ee}^{LL} - yll_{ee}\mathfrak{F}^{\max} \leq 0 \qquad \text{(B36)}$$

$$f_{ee}^{VV} - yvv_{ee}\mathfrak{F}^{\max} \leq 0, \qquad \text{(B37)}$$

and so forth.

• To ensure that utility exchangers exist only if the module exists

$$yh_e - y_e \leq 0 \qquad \text{(B38)}$$

$$yc_e - y_e \leq 0. \qquad \text{(B39)}$$

• To ensure that interconnecting streams exist only if corresponding modules exist

$$yll_{ee'} - 0.5\left[y_e + y_{e'}\right] \leq 0 \qquad \text{(B40)}$$

$$yIl_{ne} - y_e \leq 0, \qquad \text{(B41)}$$

and so forth.

• To ensure that if a module exists, there will be an inlet flow

$$y_e - \left[\sum_n yIl_{ne} + \sum_{e'} yll_{e'e} + \sum_{e'} ycl_{e'e}\right] \leq 0 \qquad \text{(B42)}$$

$$y_e - \left[\sum_{e'} yvv_{e'e} + \sum_{e'} yhv_{e'e}\right] \leq 0, \qquad \text{(B43)}$$

and so forth.

• To ensure that if a module exists, there will be an outlet flow

$$y_e - \left[\sum_{e'} yll_{ee'} + \sum_{e'} ylh_{ee'} + \sum_p ylp_{ep}\right] \leq 0 \qquad \text{(B44)}$$

$$yc_e - \left[\sum_{e'} ycl_{ee'} + \sum_p ycp_{ep}\right] \leq 0, \qquad \text{(B45)}$$

and so forth.

• To ensure at least one feed point per existing feed $n \in I1$

$$1 - \left[\sum_e yIl_{ne} + \sum_e yIh_{ne} + \sum_p yIp_{np}\right] \leq 0. \qquad \text{(B46)}$$

• To ensure at least one source per product $p \in P$

$$1 - \left[\sum_n yIp_{np} + \sum_e ylp_{ep} + \sum_e ycp_{ep}\right] \leq 0. \qquad \text{(B47)}$$

• To define the utilization of an entrainer $n \in I2$

$$y\,\mathrm{solv}_n - \left[\sum_e yIl_{ne} + \sum_e yIh_{ne} + \sum_p yIp_{np}\right] \leq 0. \qquad \text{(B48)}$$

• Nonredundancy constraints, since all modules are the same

$$y_{e+1} - y_e \leq 0. \qquad \text{(B49)}$$

10. Objective function: Synthesis of the separation system may be driven by

• Maximization of the molar fraction of a component C in a product stream (that is, separation efficiency), or

• Minimization of a cost function, involving

Utility cost

$$\mathrm{Cost}^{\mathrm{util}} \sum_e \left(Qh_e + Qc_e\right).$$

Entrainer cost

$$\mathrm{Cost}^{I2} \sum_{I2} f^{I2}.$$

''Pseudocapital'' cost of each module, which may be a fixed cost or a function of stream flows and/or separation efficiency.

The basic assumptions listed in the second section can be easily relaxed within this framework as follows. To consider liquid and vapor states of feeds and products, their corresponding interconnections must also be considered, that is, in addition to the stream sets listed earlier, account for the following sets;

IV_{ne} = {s/s interconnecting stream from initial stream n to vapor inlet mixer of module e}

IC_{ne} = {s/s interconnecting stream from initial stream n to utility cooler of module e}

VP_{ep} = {s/s interconnecting stream from vapor outlet splitter of module e to final mixer of product p}

HP_{ep} = {s/s interconnecting stream from utility heater of module e to final mixer of product p}.

The superstructure model can then be appropriately altered. To consider variable system pressure, a variable pressure is assigned to each stream or to each module. To include heat exchangers without phase change, the building-block module of Figure 2b can be modified to that shown in Figure B1, whereby three coolers and three heat exchangers are connected to the mass/heat exchanger. All heating and cooling possibilities are considered, accompanied by the in-

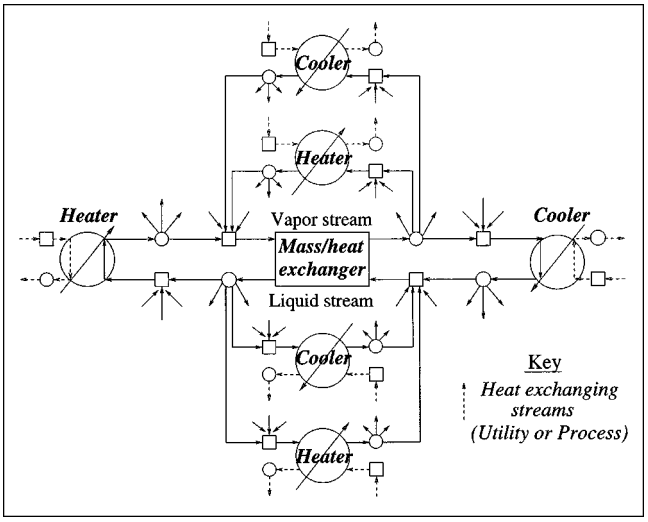

Figure B1. Complex heat-exchange module.

creased complexity of the model. Heat integration can be considered by accounting for utility and process streams to exchange heat. However, the problem is simplified to disregard heat integration when the dashed lines are utility streams.

Appendix C: Solution Strategy

The mass/heat-exchange superstructure model, presented in detail in the fifth section, can be recast in the following compact mathematical form (model P):

$$
\begin{array}{lll}
\min & f(x, y^s, y^t) & \\
\text{s.t.} & h(x) = 0 & \text{mass and energy balances} \\
 & g_1(x, y^s, y^t) \le 0 & \text{mass driving-force constraints} \\
(\text{P}) & & \text{stream characterization,} \\
 & & \quad \text{and so forth} \\
 & g_2(x, y^s) \le 0 & \text{existence of modules/blocks} \\
 & & \quad (\text{flows, mass transferred, etc.}) \\
 & g_3(y^s) \le 0 & \text{structural constraints,}
\end{array}
$$

where

x = continuous variables
y^s = structural binary variables
y^t = binary variables for mass transfer direction.

(P) is a large-scale MINLP problem. We propose the following nested decomposition for its solution (see Figure C1).

Decomposition

- Primal Problem: by fixing y^s and y^t. It provides an upper bound to the overall solution of (P).
- Inner Master Subproblem: by fixing y^s; determines y^t.
- Outer Master Subproblem: determines both y^s and y^t and provides a lower bound to the overall solution of (P).

The detailed formulation follows:

1. Primal Problem k

$$
\left.
\begin{array}{lll}
U^k = \min & f(x, y^s_{k1}, y^t_k) & \\
\text{s.t.} & h(x) = 0 & \\
 & g_1(x, y^s_{k1}, y^t_k) \le 0 & \\
 & g_2(x, y^s_{k1}) \le 0 &
\end{array}
\right\}
\begin{array}{c}
\text{Upper bound } U^k \\
\& \\
\text{Lagrange multipliers} \\
\lambda_1^{k(k1)}, \lambda_2^{k(k2)},
\end{array}
$$

where

$$
k \text{ corresponds to} = \begin{cases} k1, & \text{outer iteration} \\ k2, & \text{inner iteration,} \end{cases}
$$

that is, $k = 1, \ldots, k2(k1)$.

2. Inner Master Subproblem k2

$$
\begin{array}{ll}
\min & \mu \\
\text{s.t.} & \mu \ge f(x^{k2}, y^s_{k1}, y^t) + \sum_{k2} \lambda_1^{k2} g_1(x^{k2}, y^s_{k1}, y^t) \\
 & \qquad k2 = 1, \ldots, k2(k1)_{\text{fesible}} \\
 & \qquad (\text{that is, only from primals of current } y^s_{k1}) \\
 & \sum_{k2} \lambda_1 g_1(x^{k2}, y^s_{k1}, y^t) \le 0 \\
 & \qquad k2 = 1, \ldots, k2(k1)_{\text{infeasible}} \\
 & + \text{integer cuts for transfer direction } y^t \text{ that} \\
 & \quad \text{have been examined in current outer iteration } k1.
\end{array}
$$

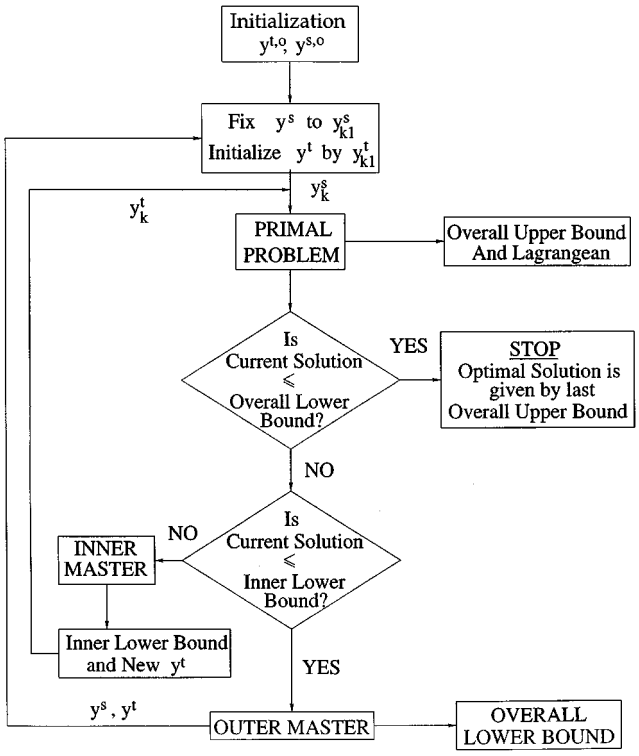

Figure C1. MINLP decomposition algorithm.

The solution of the inner master subproblem provides a lower bound to the solution of the primal problem with *fixed* current structure.

3. Outer Master Subproblem k1

$$\min \quad \mu$$

$$\text{s.t.} \quad \mu \geq f\left(x^{k2(k1)}, y^s, y^t\right) + \sum_k \lambda_1^{k2(k1)} g_1\left(x^{k2(k1)}, y^s, y^t\right) + \sum_k \lambda_2^{k2(k1)} g_2\left(x^{k2(k1)}, y^s\right)$$

$$\forall \quad k = k2(k1) \text{ feasible primal}$$

$$\sum_k \lambda^{k2(k1)} g_1\left(x^{k2(k1)}, y^s, y^t\right) + \sum_k \lambda_2^{k2(k1)} g_2\left(x^{k2(k1)}, y^s\right) \leq 0$$

$$\forall \quad k = k2(k1) \text{ infeasible primal}$$

$$g_3\left(y^s\right) \leq 0$$

+ integer cuts for combinations of structure and transfer directions that have already been examined (that is, including y^s, y^t).

The solution of the outer master subproblem provides a valid lower bound to the *overall* solution of problem (P).

Remarks

1. The inner iterations can stop when a feasible mass-transfer pattern is found.
2. Integer cuts in the outer master subproblem *must* involve both structural and transfer binary variables when inner iterations stop before convergence. This is required so that a structure with a better y^t than the ones examined is not rejected. When, for a given structure y^s, the best y^t is found, then an integer cut for the structure can also be included.
3. The outer master subproblem must involve variable y^t to provide a valid lower bound.
4. Common assumptions for convexity are required to ensure convergence to the optimal solution.
5. Convergence in a finite number of iterations is guaranteed since only a finite number of combinations exist.

Appendix D: Model Size Statistics

The size of the superstructure model as detailed in the fifth section is given in Table D1, expressed in terms of the number of mass/heat-transfer blocks e, components in the system c, initial streams i, and product streams p.

Table D1. MINLP Model Size

	Example 1 Ethanol & Water	Example 2 Acetone & Chloroform
Primal (NLP)		
Continuous variables	$6e^2+16e+14ec+2ep+6pc+6ec^2+6pc^2+2p+i(e+p+2)+1$	$6e^2+16e+15ec+2ep+7pc+2ec^2+2pc^2+2p+i(e+p+2)+1$
Equalities		
• Properties	$6ec^2+6pc^2+32ec+8pc+ic$	$2ec^2+2pc^2+33ec+9pc+ic$
• Balances, etc.	$21e+5ec+i+3p+pc$	
Inequalities	$6e^2+14e+6ec+2ep+ie+ip+p$	
Outer Master Problem (MIP)		
Binary variables	$3e+i+ie+ip+2ep+6e^2+ec$	
Equations	$6e^2+9e+ie+ip+2ep+i+p+6$	

The synthesis model for the separation of acetone and chloroform involves 2,210 continuous variables (of which 1,170 are thermodynamic variables) and 2,704 equations in the primal (1,544 equalities; 1,160 inequalities), and 778 binary variables and 861 equations in the outer master problem. The first structure (Figure 16) was a result of two outer iterations and four inner iterations obtained in 381 CPU seconds, while the second structure (Figure 18) was a result of four outer iterations and seven inner iterations, taking 520 CPU seconds.

The overall synthesis task for the separation of ethanol and water (tasks 3 and 4) involves 2,606 continuous variables (of which 1,566 are thermodynamic variables) and 3,100 equations (1,940 equalities; 1,160 inequalities) in the primal and 778 binary variables (including structural binaries for interconnections) and 861 equations in the outer master problem.

The final structure for task 3 was obtained in three outer master iterations and five inner master iterations (424 CPU seconds), while the final structure for task 4 required four outer iterations and six inner iterations (512 CPU seconds).

The synthesis model for the separation of acetone and chloroform involves 2,210 continuous variables (of which 1,170 are thermodynamic variables) and 2,704 equations in the primal (1,544 equalities; 1,160 inequalities), and 778 binary variables and 861 equations in the outer master problem. The first structure (Figure 16) was a result of two outer iterations and four inner iterations obtained in 381 CPU seconds, while the second structure (Figure 18) was a result of four outer iterations and seven inner iterations, taking 520 CPU seconds.

Note that the binary variables in both examples correspond to 10 mass/heat exchangers, 20 pure heat exchangers, 2 possible entrainers, 40 mass-transfer directions (possible 4 components in each block), and 706 interconnections.

Manuscript received May 11, 1998, and revision received Apr. 26, 1999.